Student Research Accomplishments 2006 - 2007

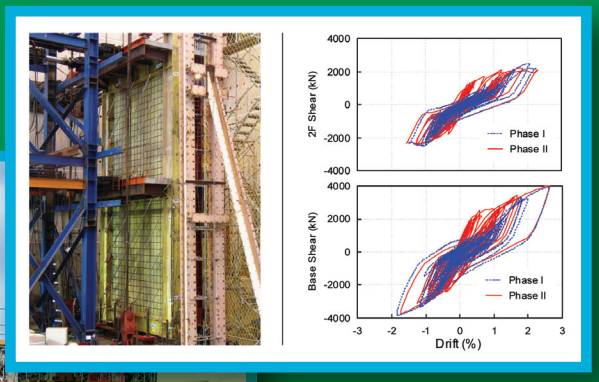

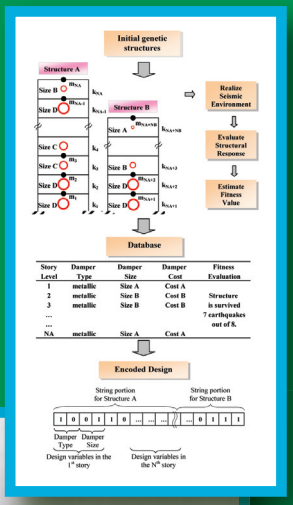

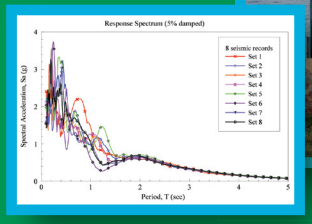

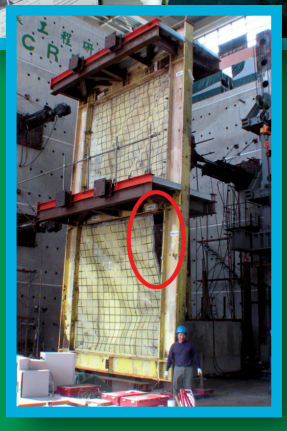

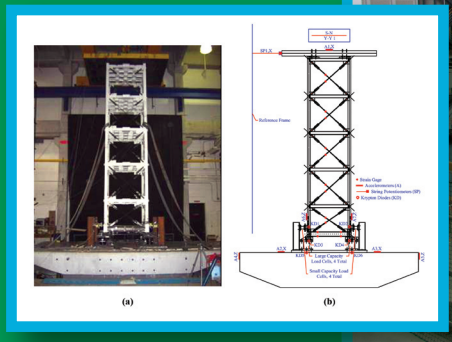

MCEER
EARTHQUAKE ENGINEERING TO EXTREME EVENTS

November 2007

MCEER

MCEER is a national center of excellence in advanced technology applications that is dedicated to the reduction of earthquake losses nationwide. Headquartered at the University at Buffalo, State University of New York, the Center was originally established by the National Science Foundation (NSF) in 1986, as the National Center for Earthquake Engineering Research (NCEER).

Comprising a consortium of researchers from numerous disciplines and institutions throughout the United States, the Center's mission is to reduce earthquake losses through research and the application of advanced technologies that improve engineering, pre-earthquake planning and post-earthquake recovery strategies. Toward this end, the Center coordinates a nationwide program of multidisciplinary team research, education and outreach activities.

Funded principally by NSF, the State of New York and the Federal Highway Administration (FHWA), the Center derives additional support from the Federal Emergency Management Agency (FEMA), other state governments, academic institutions, foreign governments and private industry.

Student Research Accomplishments

2006-2007

MCEER
University at Buffalo, State University of New York

Edited by Seda Dogruel and Rodrigo Retamales

November 2007

MCEER-07-SP05

Red Jacket Quadrangle, Buffalo, New York 14261
Phone: (716) 645-3391; Fax: (716) 645-3399
E-mail: *mceer@mceermail.buffalo.edu*
World Wide Web: *http://mceer.buffalo.edu*

Foreword

The Student Leadership Council (SLC) is a formal incarnation of the students who are involved in performing MCEER research under a faculty advisor. Since its inception, MCEER has included and encouraged student efforts throughout its research program and in all of the disciplinary specialties concerned with earthquake engineering.

Throughout the years, students have been an integral component in advancing research in earthquake hazard mitigation. Many former students are now employed in academia, professional practice or government agencies, applying knowledge gained during their exposure to MCEER research. While associated with MCEER, students participate in Center annual meetings, attend conferences, workshops and seminars, and have the opportunity to make presentations at these events. The SLC was formed in the year 2000 to formalize these programs and to afford students from many different institutions the opportunity to meet with each other and develop/improve interaction.

The idea for the *Student Research Accomplishments* was conceived by the SLC and features the work of MCEER's current students. Topics range from traditional civil and lifeline engineering to applications of advanced technologies to social impacts and economic modeling.

This volume was coordinated and edited by Seda Dogruel and Rodrigo Retamales, Ph.D. Candidates, University at Buffalo. Previous editors were Navid Haji Allahverdi Pur, from the New Jersey Institute of Technology, Amanda Bonneau, from Cornell University, Mike Pollino, Ramiro Vargas, Benedikt Halldorsson, and Diego Lopez Garcia, all from the Department of Civil, Structural and Environmental Engineering, University at Buffalo, and Gauri Guha, Department of Energy, Environmental and Mineral Economics, the Pennsylvania State University.

Finally, MCEER wishes to extend its thanks to the Student Leadership Council for its endeavors, and in particular to Michael Pollino, Jeffrey Berman, and A. Natali Sigaher, past presidents, for their able guidance of the SLC.

Contents

1

Seismic Resilience of a Regional System of Hospitals

Gian Paolo Cimellaro

Graduate Research Assistant, Department of Civil, Structural and Environmental Engineering, University at Buffalo

Advisors: Andrei M. Reinhorn, Professor and Director of NEES and Michel Bruneau, Professor and Director of MCEER

Summary

The concepts of seismic resilience and its quantitative evaluation are presented. The evaluation is based on non-dimensional analytical functions related to loss variation within a specified "recovery period", recovery function and fragility functions. The path to recovery usually depends on available resources and may take different shapes which can be estimated by proper recovery functions. Loss functions include both direct and indirect losses that are uncertain in themselves due to the uncertain nature of earthquake and structural behavior as well as due to uncertain description of functional limit states. Therefore, losses are functions of fragility of systems' components that are determined and combined together through use of multidimensional performance limit thresholds. The formulated framework is applied and exemplified for a complex system of six hospitals located in Memphis Tennessee, considering direct and indirect losses in its physical system and in the population served by the system. The example presented shows that for high system functionality values Q(t), the marginal recovery cost doubles the cost associated to lower functionality values.

Introduction

MCEER performance assessment methodology (Resilience) is primarily developed to improve decision making procedures with regards to seismic performance of facilities and systems in general. In MCEER terminology, Seismic Resilience is a decision variable (*DV*) and a quantifiable measure of seismic performance that describes the recovery from a given loss required to maintain the function of the system with minimal disruption. Seismic resilience framework can compare losses and different pre and post event measures in order to verify if strategies and actions can reduce or eliminate disruptions in presence of seismic events. In previous studies, Bruneau et al., (2003) defined a fundamental framework for evaluating community resilience without any actual quantification and implementation. They offered a very broad definition of resilience to cover all actions that reduces losses from hazard, including mitigation and more rapid recovery. Chang et al., (2004) proposed a series of quantitative measures of resilience and applied them to a case study of an actual community, the seismic mitigation of the Memphis water system. Researchers at MCEER have developed a framework equation on the basis of concept of conditional probability and total probability theorem that attempts to provide a quantitative definition of resilience (Cimellaro et al., 2006b). In this paper the formulated framework is applied and exemplified for a complex system of six hospitals located in Memphis, Tennessee.

Analytical formulation

In order to obtain a realistic quantification of the uncertainties of Resilience, various sources of uncertainties are incorporated in the framework equation. They are related to losses, function of

recovery and time of recovery and combined in a unique quantity called "Resilience". In this framework the following uncertainties are considered and modelled as random variables: (a) uncertainties of the ground motion; (b) uncertainties of the structural response; (c) uncertainties of the limit states; (d) uncertainties in the estimation of the losses; (e) uncertainties in the estimation of the time of Recovery (Tre) and (f) uncertainties in the function of recovery. All these information are summarized in Equation (1) and visualized in Figure 1:

$$\overline{R}=\frac{1}{N_I}\sum_{I=1}^{N_I}\left\{\frac{1}{N_E}\sum_{E=1}^{N_E}\frac{1}{T_{RE}}\int_{t_{0E}}^{t_{0E}+T_{RE}}\left\{1-L(I,T_{RE})\left[H(t-t_{0E})-H(t-(t_{0E}+T_{RE}))\right]\alpha_R f_{Rec}(t,t_{0E},T_{RE})\right\}dt\; p_E(0,T_{LC})\right\}P(I) \qquad (1)$$

where N_E is the number extreme events expected during the lifespan (or control period) T_{LC} of the system, N_I is the number of different extreme events intensities expected during the lifespan (or control period) T_{LC} of the system; T_{RE} is the recovery time from event E; t_{0E} is the time of occurrence of event E; $L(I,T_{RE})$ is the normalized loss function; $f_{REC}(t, t_{0E}, T_{RE})$ is the recovery function; $P(I)$ is the Probability that an event with intensity I happens in a given time interval T_{LC}; $p_E(0,T_{LC})$ is the probability that an event happens E times in a given time interval T_{LC}; α_R is a recovery factor and $H(t_0)$ is the Heaviside step function. In equation (1) there are the loss function $L(I,T_{RE})$, the recovery function $f_{REC}(t,t_{0E},T_{RE})$ and the fragility function that does not appear explicitly, but it is included in the loss function that will be defined in the following section.

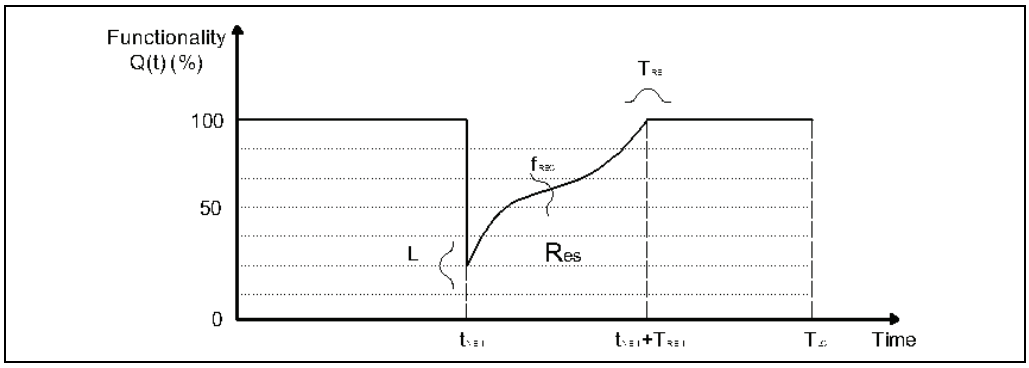

Figure 1. Resilience

Case study: complex of six hospitals located in Memphis

To illustrate the proposed framework equation a complex of six hospitals located in Memphis, Tennessee has been used (Figure 2). It consists of a regional loss estimation study aimed at the estimation of economic losses of several buildings within a geographical region like a city. Figure 2 shows the locations (by Zip code) that are used to define the seismic Hazard (U.S.G.S. 2002) and the structural type of the hospitals that are used to define the structural vulnerability (HAZUS 2005). Four seismic rehabilitation alternative schemes are considered for each structural type: 1) *no action*; 2) *rehabilitation to life safety level*; 3) *rehabilitation to immediate occupancy level*; 4) *construction of a new building*. These rehabilitation levels are, as defined in FEMA 276 (1999), the target performance levels for rehabilitation against an earthquake. The initial rehabilitation costs for the options considered here are obtained from FEMA 227 (1992) and FEMA 156 (1995), which provide typical costs for

rehabilitation of existing structures taking into account many factors, such as building type, earthquake hazard level, desired performance level, occupancy or usage type.

Fragility curves for each rehabilitation alternative (as defined in FEMA 276) are obtained directly correlating to the HAZUS code levels. Therefore, the HAZUS code levels are assigned to the rehabilitation levels mentioned above with reasonable assumptions (e.g. it is assumed that the "No Action" option, corresponds to the low code level). Fragility curves are developed for structural damage and nonstructural damage of drift sensitive and accelerations sensitive components using the HAZUS approach. Then fragility curves are combined together using the multidimensional fragility approach (Cimellaro et al. 2006a). Figure 3 shows fragility curves of structural damage for concrete shear walls mid rise building type (C2M). They are plotted for different damage states and are function of earthquake intensity measures that in this case is considered in term of return period.

The time control period T_{LC} for a decision analysis is based on the decision maker's interest in evaluating the alternatives. Generally, building system rehabilitation is better justified with longer time period, because the expected seismic losses associated with seismically vulnerable structure increases with longer time period. On the other hand a decision maker would feel more favorable to rehabilitation of structures when the rehabilitation is justified with shorter time period. Therefore, the time control period of the system T_{LC} is assumed to be 30 years and a discount annual rate r of 6% is assumed. Figure 4 shows a comparison of structural damage distributions for two time control periods T_{LC}=30 yrs and T_{LC}=50 yrs for C2M type structures. As expected the probability of having no damage increases with shorter time periods.

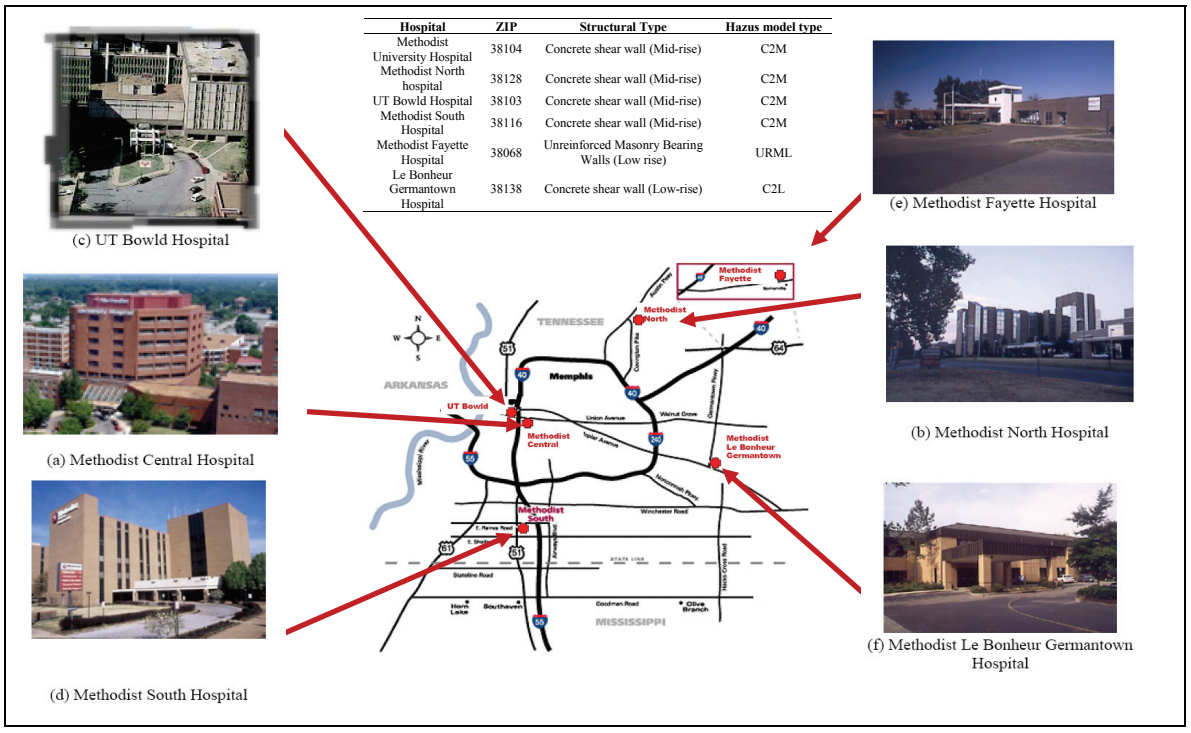

Figure 2. System definition (Park, 2004)

Using the damage probability distributions (Figure 4), various seismic losses associated with the system are estimated using HAZUS approach (Table 1). It is assumed that losses of different

hospitals units are independent, so the total loss of the system can be obtained by simply adding different losses. Then, losses (L) are combined using the approach described in Cimellaro et al., (2006b) and recovery time (T_{RE}) are estimated for the four earthquake levels and loss hazard curves are generated to calculate the overall expected loss. The values of seismic resilience are calculated according to Equation (1) for different damage states that are function of the seismic input.

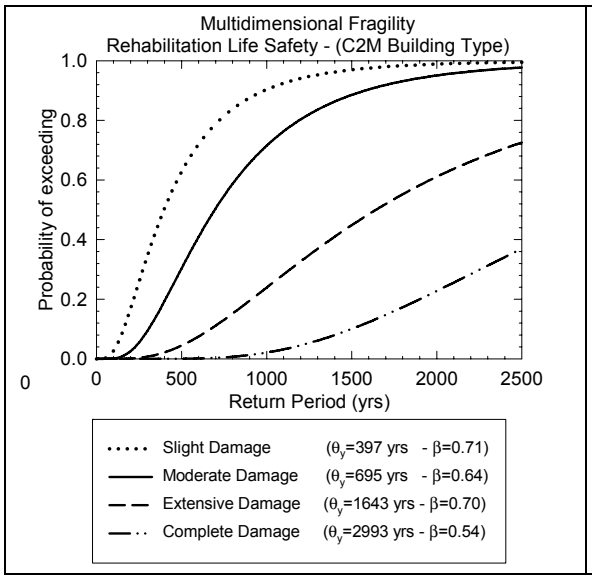

Figure 3. Multidimensional fragility curves for C2M type structure -Rehabilitation to Life Safety

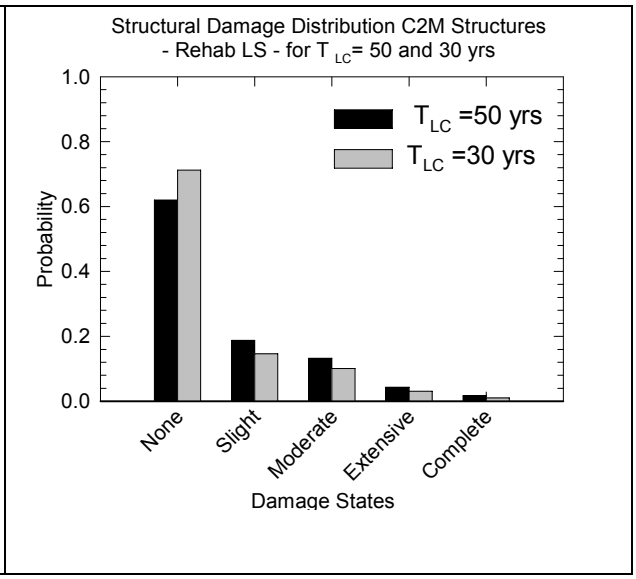

Figure 4. Structural damage distribution for different rehabilitation strategies (T_{LC}=30 yrs) for C2M type structure - Rehabilitation to Life Safety

Table 1. Normalized losses for different Damage States of C2M buildings (HAZUS, 2005)

		Slight	Moderate	Extensive	Complete	Complete [$/ft^2]
LS	**Structural Repair Cost**	0.0176	0.1	0.5	1	17
LNS,DE	**Drift Sensitive nonstructural Cost**	0.0190	0.1	0.5	1	42
	Acceleration Sensitive nonstructural Cost	0.0194	0.1	0.3	1	62
	Contents Loss	0.020	0.1	0.5	1	60.5
LNS,DC	**Death**	0	0	0.000015	0.125	
	Injury	0	0.0003	0.001005	0.225	
	Recovery Time (days)	2	67.5	270	360	

In order to get rid of the seismic input its value is normalized using the four different hazard levels considered in this case. After normalization the values can be evaluated for different rehabilitation strategies (Figure 5).

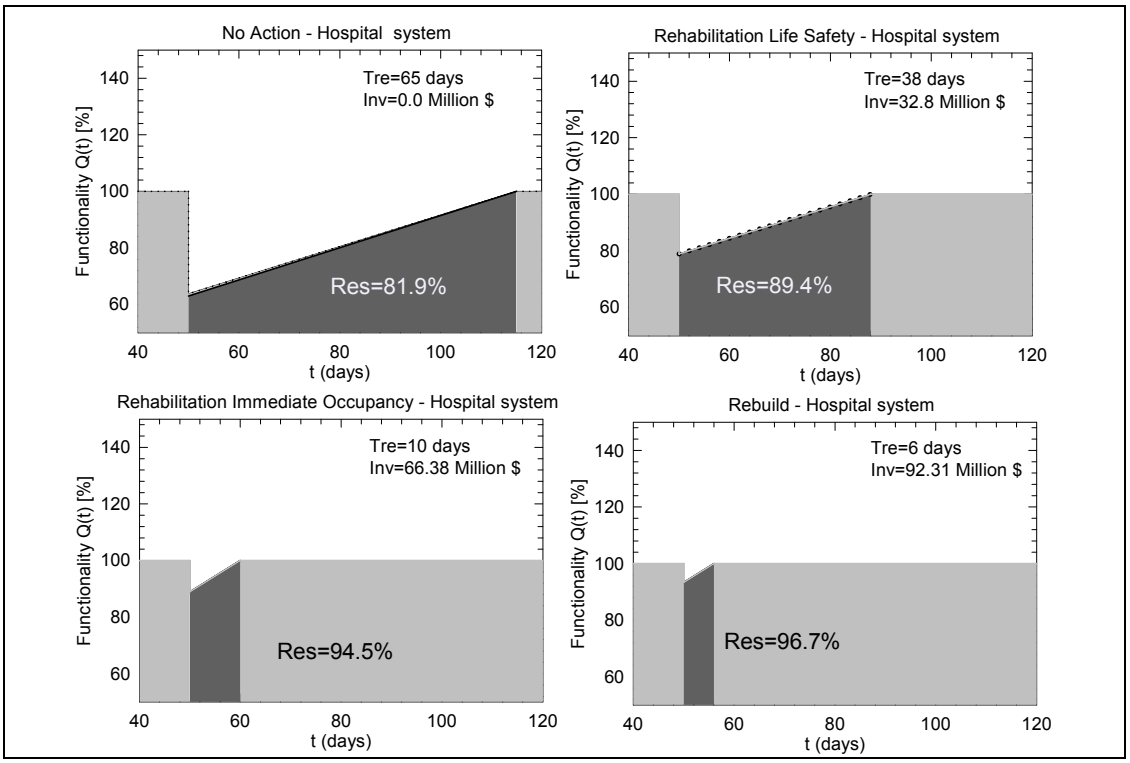

Figure 5. Resilience for different rehabilitation strategies

Table 1. Rehabilitation costs, Recovery time and Seismic Resilience for different rehabilitation strategies.

Rehabilitation Alternatives	Rehabilitation Costs [$ Million]	Expected earthquake Loss [$ Million]	Total Costs* [$ Million]	Recovery Time T_{RE} [days]	Resilience Res [%]
No Action	0	32.34	119.64	65	81.9
Life Safety (LS)	32.8	18.86	138.96	38	89.4
Immediate Occupancy (IO)	66.38	9.54	163.22	10	94.5
Rebuild	92.31	5.82	185.43	6	96.7

The initial costs of rehabilitation for different rehabilitation strategies, the average recovery time and resilience values are summarized in Table 1. For this case study it is shown that the *Rebuild Option* is able to obtain the biggest value of seismic Resilience (96.7%) if compared with the other three

* It includes cost of the entire system (87.3 Million $) + cost of rehabilitation + cost of loss recovery

rehabilitation strategies (Table 1), but it is also the most expensive solution (92.31 millions $). However, if No Action is taken the value of seismic resilience is still reasonable high (81.9%). As shown in this case study initial investments and resilience are not linearly related. When the functionality Q(t) is very high in order to improve it of small percentage is necessary to invest a huge amount of money respect to the case when the functionality of the system is low.

Concluding Remarks

The definition of seismic resilience combines information from technical and organizational fields, from seismology and earthquake engineering to social science and economics. So it is clear that many assumptions and interpretations are found to be made in the study of seismic resilience, but the final goal is to integrate the information from these different fields into a unique function leading to results that are unbiased by uninformed intuitions or preconceived notions of risk. The goal of this paper is to provide a quantitative definition of resilience in a rational way through the use of an analytical function that may fit both technical and organizational issues. A regional complex of six hospitals has been used to illustrate the applicability of the framework. The example shows that double the amount of money to improve resilience of 5.1% from 89.4% to 94.5% should be invested to improve resilience of 1.2% from 94.5 to 96.7%. However, it is important to note that the assumptions made herein are only representative for the case presented. For other problems users calculating resilience are advised to focus on the assumptions that mostly affects the problem at hand.

Acknowledgements

This research was carried out under the supervision of Andrei M. Reinhorn and primarily supported by the Earthquake Engineering Research Centers Program of the National Science Foundation under Award Number EEC-9701471 to MCEER. Any opinions, findings and conclusions or recommendations expressed in this paper are those of the author(s) and do not necessarily reflect those of the NSF or NYS.

References

Bruneau, M., Chang, S., Eguchi, R., G. Lee, O'Rourke, T., Reinhorn, A. M., Shinozuka, M., Tierney, K., Wallace, W., and Winterfelt, D. V. (2003)" A framework to Quantitatively Assess and Enhance the Seismic Resilience of Communities. *EERI Spectra Journal*, 19(4), 733-752.

Chang, S., Shinozuka M. (2004): Measuring Improvements in the disaster Resilience of Communities, *EERI Spectra Journal*, 20, (3), 739-755.

Cimellaro, G. P., Reinhorn, A. M., Bruneau, M., and Rutenberg, A. (2006a): Multidimensional Fragility of Structures: Formulation and Evaluation. *Report MCEER-06-0002, pp. 123*, Multidisciplinary Center for Earthquake Engineering Research, Buffalo, NY.

Cimellaro, G. P., Reinhorn, A. M., and Bruneau, M. (2006b): Quantification of Seismic Resilience. *Proceedings of the 8th National Conference of Earthquake Engineering*, paper 1094, San Francisco, California, April 18-22.

FEMA. (1999). "Example Applications of the NEHRP Guidelines for the Seismic Rehabilitation of Buildings." FEMA 276, Federal Emergency Management Agency and U.S. Army Corps of Engineers, Washington D.C.

FEMA. (1995). "Typical Costs for Seismic Rehabilitation of Existing Buildings, Vol 1 – Summary." FEMA 156, Federal Emergency Management Agency and U.S. Army Corps of Engineers, Washington D.C.

FEMA. (1992). "A Benefit-Cost Model for the Seismic Rehabilitation of Buildings." FEMA 227, Federal Emergency Management Agency and U.S. Army Corps of Engineers, Washington, DC.

HAZUS. (2005). "FEMA`s Software Program for Estimating Potential Losses from Disasters-Technical Manual." Washington D.C.

Park, J. (2004): Development and application of probabilistic decision support framework for seismic rehabilitation of structural systems. *Ph. D. Dissertation,* Georgia Institute of Technology, *U. S. A*, November 2004.

U.S.G.S. (2002). "National Seismic Hazard Mapping project, Version 2002." http:/eqint.cr.usgs.gov/eq/html/lookup-2002-interp.html.

2

Evolutionary Seismic Design and Retrofit with Application to Adjacent Structures

Seda Dogruel

Ph.D. Candidate, Department of Civil, Structural and Environmental Engineering, University at Buffalo

Advisor: Gary F. Dargush, Professor

Summary

Although passive control devices have been widely used for the seismic retrofit of existing structures, current design codes do not provide guidelines for optimizing configuration of dampers or choosing the appropriate device type that may enhance the structure performance or reduce the overall design cost. In this paper, an adaptable and practical optimization methodology for seismic design of adjacent buildings is introduced using Genetic algorithms. Within the overall algorithm, passively damped structural designs evolve toward configurations that satisfy constraints on inter-story drift, absolute floor acceleration, and separation between the adjacent structures while attempting to limit damper cost. It is suggested that the methodology presented in this paper can achieve significant improvements in determination of the optimum distribution, number, and/or size of passive-control devices of known capacity in adjacent buildings and can provide a powerful approach for mitigating potential damage due to pounding.

Introduction

Over the past decades, pounding between adjacent buildings has been observed during most major urban earthquakes (Filiatrault A. et al. 1994; Kasai and Maison, 1997). A sufficient separation between the structures would avoid the structural pounding; however, for metropolitan cities located in regions of high seismic activity, the need to maximize use of land has lead to inadequate separation often resulting in pounding of adjacent structures during a strong earthquake. Intensive study has been carried out on mitigation techniques of structural pounding hazards by applying different structural models and using various models of collisions (Anagnostopoulos 1995; Lopez Garcia 2004). Seismic design of adjacent buildings, retrofitted with passive-control devices, is one of the suggested pounding mitigation methods and is reasonably applicable to optimization techniques. Location, type, size, and number of dampers can be design variables when considering an optimized seismic design of adjacent buildings. The model of searching in a large design space, theoretically formed by combining all possible values of the design variables, may be difficult to formalize mathematically or expensive to compute. Therefore, recently, tracing a path through increasingly "better" designs has become a realistic perspective for many researchers. Genetic algorithms (GAs), which were originally developed by Holland (1975), are one of the efficient search algorithms based on the evolutionary theory of "survival of the fittest". GAs have the robustness and the capability to perform well over a wide range of problems. Thus, many researchers (Furuya et al. 1998, Singh and Moreschi 2002; Dargush and Sant 2005) used GAs for the optimum seismic design of structures. In this paper, the evolutionary seismic design and retrofit approach defined in Dargush and Sant (2005) is extended for adjacent structures. With minimum cost and maximum functionality objectives, a

general computational framework that promotes evolution of robust seismic design and retrofit of adjacent structures subjected to fixed seismic environments is developed.

Seismic Design Procedure

A uniaxial version of a two-surface cyclic plasticity model (Chopra and Dargush 1994) is implemented for the nonlinear transient dynamic analysis with an explicit state-space approach for the primary structures and metallic yielding dampers. Primary structures simplified by lumped parameter models may contain a number of metallic yielding dampers, viscoelastic solid dampers and/or viscous fluid dampers. A coupled thermo-viscoelastic Maxwell model is used for viscoelastic dampers. Additionally, viscous fluid dampers are modeled as strictly linear Newtonian devices. Details on the mathematical models employed for passive energy dissipation devices can be found in Dargush and Soong (1995), Constantinou et al. (1998).

Seismic environment is characterized in a manner consistent with the Multidisciplinary Center for Earthquake Engineering Research (MCEER) Northridge Earthquake ensemble (2% PE in 50 years) (Filiatrault and Wanitkorkul 2005). Eight ground motion records are used for the fixed seismic environment analysis. The peak ground acceleration (PGA), the peak ground velocity (PVG), the peak ground displacement (PGD) amplitudes, and the period corresponding to the intersection of the constant spectral acceleration and constant spectral velocity branches of a 5% damped elastic spectrum, $T_{V/A}$ values of these eight ground motion records are listed in Table 1 and Figure 1 shows the 5% damped spectrum of the records of Table 1.

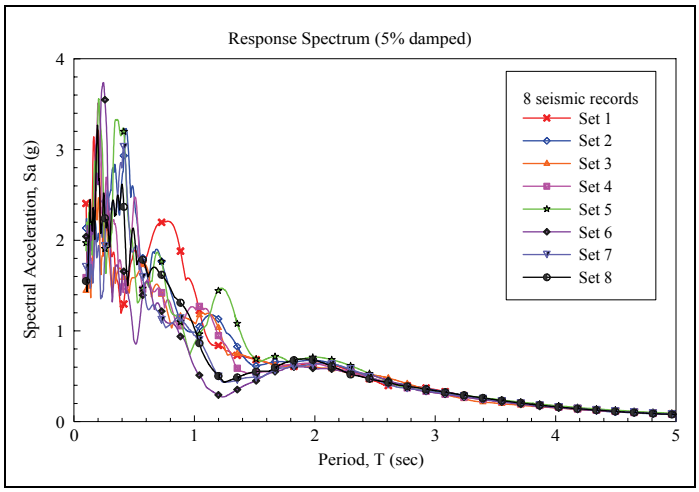

Figure 1. 5% damped spectrum of the records of Table 1

Table 1. Eight ground motion records from MCEER Northridge earthquake ensemble

	Set 1	Set 2	Set 3	Set 4	Set 5	Set 6	Set 7	Set 8
PGA [g]	1.25	0.94	0.79	0.79	0.97	0.85	0.82	0.86
PDV [m/sec]	0.83	0.93	0.99	0.96	0.98	0.69	0.97	1.03
PGD [m]	1.00	0.44	0.48	0.45	0.40	0.40	0.71	0.65
$T_{V/A}$ [sec]	0.33	0.49	0.63	0.61	0.50	0.40	0.59	0.60

Performance Based Evolutionary Optimization

This study develops an automated performance based design algorithm that can identify the optimized design or retrofit of both single and adjacent structures under fixed seismic environments. Figure 2 illustrates the overall process of constructing the GA string representation generated for a pair of adjacent steel frame structures. GA starts with a set of initial pair of structural designs that are generated from an exhaustive combination of different damper sizes and/or types. Within each generation, each structure is subjected to a specified number of seismic environmental conditions and evaluated to determine the degree to which the objective is satisfied and to what extent design constraints are violated. Violation is also possible during other seismic events for that individual within the current generation. Consequently, as shown in Figure 2, each evaluation involves the realization of the structure and appropriate ground motions. The fitness values, along with random genetic operators modeling selection, crossover, and mutation processes, define the framework of the next generation of structures.

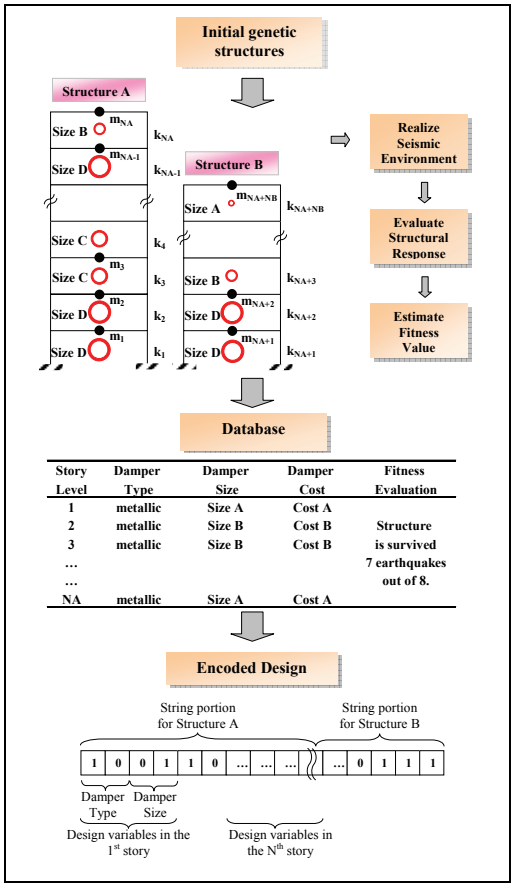

Figure 2. Overall framework of evolutionary methodology

Objective Criteria: Minimum damage to the structure under seismic loading is certainly the most desirable performance criteria for the seismic design or retrofit of structures. In order to quantify the damage to the structure, the relationship between validation of design constraints and degree of damage should be established. Not satisfying the drift or acceleration or separation design constraints for a given earthquake excitation, is assumed to directly lead to design failure. Thus, the degree of damage to a structure can be formulized with the use of survival rate that the proposed design realized (i.e., the ratio of earthquake survivals to total number of earthquake attempts). As well as minimizing the damage to structure, minimizing the overall structural cost is another significant design objective. The mathematical formulation of a meaningful cost definition is achieved by using relative realized cost and size values for dampers, assuming that the cost of any type of damper is proportional to its size. The foregoing two performance criteria, concerning overall structural cost and structural damage are combined into a single objective function, which is defined as fitness function, f, for each structure. The fitness function f (also called the utility function) to be maximized is formulated in Equation 1 as follows:

$$f = \left(\frac{B-C}{B}\right)\left(1-\frac{D}{B}\right)^{r} \tag{1}$$

where B, C, and D are variables representing the economic benefit derived from the structure, the cost of passive-control devices, the damage to structure associated with the seismic environment

respectively. Additionally, the fitness function is also dependent on the risk aversion index r, which is introduced for risk-based decision making in engineering. In order to reflect the realistic evaluation of economic costs and benefits involving risk, the risk aversion index r accounts for the willingness of spending proportionally more either to avoid larger losses or to reduce epistemic uncertainties involved in the structural system, the seismic environment, and the economics.

Design Variables: The design variables are chosen to be the type of the passive control devices, the size of the passive control devices, and the cost of the passive-control devices. Therefore, there are four basic relative cost values (cost $1, 2, 3, 4$) and their associated relative size values (size $1, 2, 3, 4$) for each type of passive control devices including metallic yielding dampers, viscoelastic solid dampers, and viscous fluid dampers (e.g., the cost 1 for the size 1 viscoelastic solid damper).

Design Constraints: The primary constraints are considered to be interstory drift constraint, absolute floor acceleration constraint, and in design of adjacent structures, separation constraint in order to evaluate performance and potential damage. The allowable interstory drift is taken as 1.5% of the height of the story of the buildings (FEMA-450 2003) and the allowable absolute floor acceleration is taken to be equal to $1.5g$. Separation limit is calculated as 2.25% of the height of the story of the buildings by adopting the square root of the sum of the squares rule of the two lateral displacements of adjacent buildings (IBC 2003). Then, the performance of structural response reduction is expressed in terms of reduction in the maximum interstory drift, the maximum absolute floor acceleration and the maximum relative displacement between adjacent structures.

Computational Simulations

A series of design examples, involving a pair of undamped adjacent steel frame structures (Building A and Building B), with various retrofit possibilities are selected as an example to examine the competence of the proposed GA based automated design methodology for configuring passive-control devices in the adjacent buildings, rather than to provide guidance for specific design situations. Building A is a twelve-story, 51.2 m. height steel frame structure with discontinuity and Building B is a five-story, 17.8 m. height steel frame structure. For computational efficiency, these buildings are simplified into a system of lumped masses connected by means of springs representing the lateral stiffness of the structure. Additionally, the lumped parameter two-surface cyclic plasticity model mentioned previously is employed to represent the hysteretic behavior of the primary structures. Within this idealized model, the values of k_i, W_i, F_i^{yL}, and F_i^{yB}, representing lateral stiffness, weight, yield force on the inner loading surface, and yield force on the outer loading surface for the i^{th} story, are shown in Table 2 for Building A and Building B. The parameters listed in Table 2 are selected as $k = 172843\,\text{kN/m}$, $W = 1717\,\text{kN}$, $F^{yL} = 1718.8\,\text{kN}$, and $F^{yB} = 5156.4\,\text{kN}$. The mass and stiffness distribution of Building A is non-uniform, unlike Building B. The corresponding first natural periods for Building A and Building B are 1.5 and 0.9 seconds, respectively. The maximum structure benefit and the risk aversion index are set at $B = 2000$ and $r = 2$, respectively.

Table 2. Basic dynamic properties of the adjacent building models

	Story stiffness [kN/in]	Story weight [kN]	Yield force (inner surface) [kN]	Yield force (outer surface) [kN]
Building A	$k_1 = \ldots = k_8 = k$ $k_9 = k_{10} = 0.75k$ $k_{11} = k_{12} = 0.5k$	$W_1 = \ldots = W_8 = 1.5W$ $W_9 = \ldots = W_{12} = W$	$F_1^{yL} = \ldots = F_8^{yL} = 1.5F^{yL}$ $F_9^{yL} = F_{10}^{yL} = 1.12F^{yL}$ $F_{11}^{yL} = F_{12}^{yL} = 0.75F^{yL}$	$F_1^{yB} = \ldots = F_8^{yB} = 2F^{yB}$ $F_9^{yB} = F_{10}^{yB} = 1.5F^{yB}$ $F_{11}^{yB} = F_{12}^{yB} = F^{yB}$
Building B	$k_1 = \ldots = k_5 = 1.12k$	$W_1 = \ldots = W_5 = 1.8W$	$F_1^{yL} = \ldots = F_5^{yL} = 2F^{yL}$	$F_1^{yB} = \ldots = F_5^{yB} = 6F^{yB}$

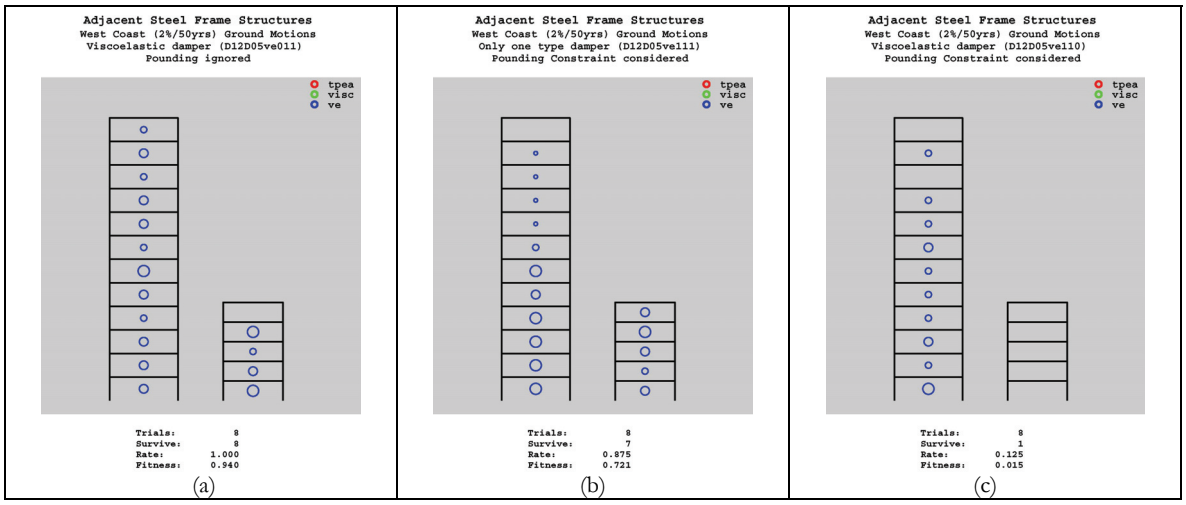

Figure 3. Twelve-story and five-story steel frames with viscoelastic dampers - robust designs with pounding (a) ignored (b) considered (c) considered but only Building A retrofitted

The seismic responses of adjacent structures, the maximum interstory drift and absolute floor acceleration, without or with passive-control devices are shown in Figure 4 and Figure 5, respectively. The maximum interstory drifts (resulted from eight different ground motions) with different passive-control device configurations are plotted in Figure 4. This figure shows that, if the dampers are uniformly distributed, the maximum interstory drift of Building A at story level eleven cannot satisfy allowable drift limit, whereas, with the proposed optimization procedure, the structural

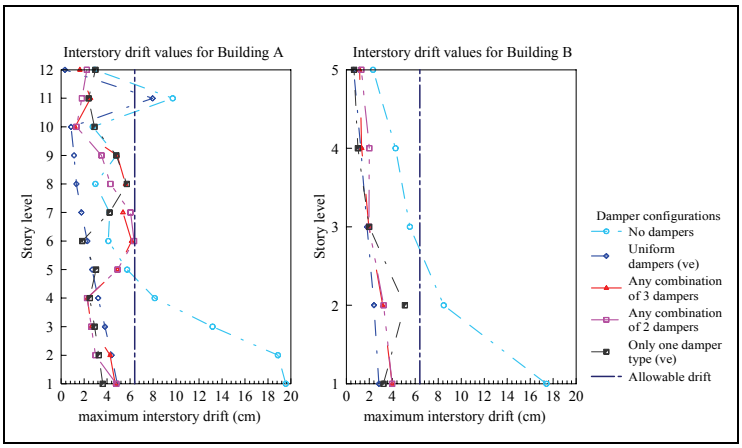

Figure 4. Maximum interstory drifts with different damper configurations

response in terms of interstory drift can

be reduced at 80% for both of the adjacent buildings, with other damper configurations. If the other seismic response, absolute floor acceleration is considered as an optimization criteria, the proposed methodology results in different values that are plotted in Figure 5. The figure shows that maximum absolute floor acceleration occurs at the ninth story of Building A. The optimization methodology can achieve a 60% reduction in absolute floor acceleration of this story level, when all three damper types are permitted for the retrofit. Note that starting from uniform to other damper configurations, accelerations are nearly same for Building A and Building B.

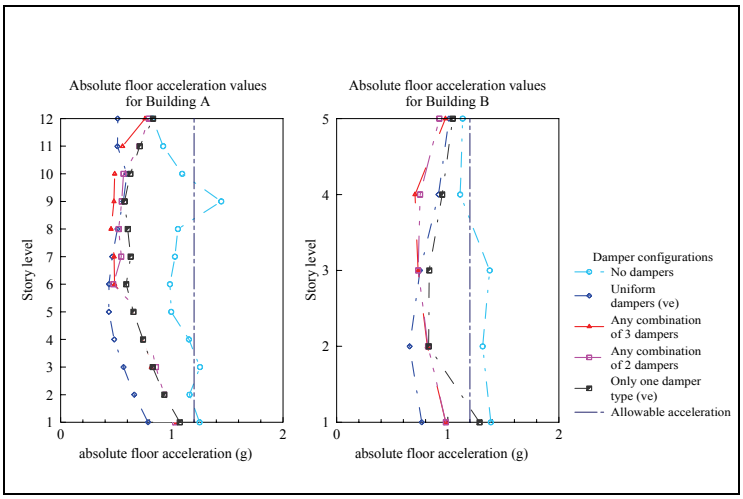

Figure 5. Absolute floor accelerations with different damper configurations

Conclusions

This paper presented a new evolutionary optimization methodology for passively controlled adjacent structures under pounding risk, based on cost and damage objectives. The method's capability of discovering robust designs was examined using a pair of adjacent structures as an example. Computational simulations of this example clearly showed that the optimal choice of the number, size, type, and distribution of the passive-control devices for the retrofit of adjacent structures often differs when potential pounding risk is ignored. The retrofit problem is complicated by the fact that, adjacent buildings usually belong to different owners, and retrofitting only one of the adjacent buildings might not be sufficient to mitigate the pounding risk.

This study is a significant attempt to encourage further research efforts that incorporate consideration of retrofitting issues of adjacent buildings under pounding risk into the structural optimization model so that the design results can be more likely applicable for a real world structural engineering practice. One of the characteristics of evolutionary algorithm appealing to researchers is its effectiveness and adaptability in handling uncertainties and nonlinearities. Because of these strengths, it is advantageous to implement the methodology to improved geophysical, structural, and even socioeconomic models. Consequently, in view of the current structural control technology, which has promising ability to provide protection to structures against multi-hazard dynamic loads, such as strong earthquakes, high winds, and/or blast loading, it is recommended that high priority of further research is given to the extension of the evolutionary algorithm to multi-hazard structural design. Research in this area, which is still in its early years, will certainly result in the enhancement of human safety and structural performance against damage by multi-hazard events.

Acknowledgement

This research was primarily supported by the Earthquake Engineering Research Centers Program of the U.S. National Science Foundation under NSF Award Number ECC–9701471. This financial support is gratefully acknowledged.

References

Anagnostopoulos S.A. (1995): Earthquake induced pounding: State of the art. Proceedings of 10th European Conference on Earthquake Engineering, 2. 897–905.

Chopra, M.B., and Dargush, G.F. (1994): Development of BEM for Thermoplasticity. *International Journal of Solid and Structures*, 31 (12/13), 1635-1656.

Constantinou, M.C., Soong, T.T., and Dargush, G.F. (1998): Passive Energy Dissipation Systems for Structural Design and Retrofit. *Monograph No.1*, Multidisciplinary Center for Earthquake Engineering Research, The State University of New York at Buffalo, Buffalo, NY.

Dargush, G.F., and Soong, T.T. (1995): Behavior of Metallic Plate Dampers in Seismic Passive Energy Dissipation Systems. *Earthquake Spectra*, 11 (4), 545-568.

Dargush, G.F., and Sant, R.S. (2005): Evolutionary Aseismic Design and Retrofit with Passive Energy Dissipation. *Earthquake Engineering and Structural Dynamics*, 34, 1601-1626.

Filiatrault, A., Cervantes, M., Folz, B., and Prion, H. (1994): Pounding of Buildings during earthquakes: a Canadian perspective. Canadian Journal of Civil Engineering; 21 (2), 251-265.

Filiatrault, A., and Wanitkorkul, A. (2005): Simulation of Strong Ground Motions for Seismic Fragility Evaluation of Nonstructural Components in Hospitals. *Technical Report MCEER-05-0005*, Multidisciplinary Center for Earthquake Engineering Research, The State University of New York at Buffalo, Buffalo, NY.

FEMA 450 (2003): *NEHRP Recommended Provisions and Commentary for Seismic Regulations for New Buildings and Other Structures*. Building Seismic Safety Council for the Federal Emergency Management Agency, Washington, DC.

Furuya, O., Hamazaki, H., and Fujita, S. (1998): Study on proper distribution of storey-installation type damper for vibration control of slender structures using genetic algorithm. *Proc., 1998 ASME/JSME Joint Pressure Vessels and Piping Conf.*, Vol. 364, San Diego, 297–304.

Holland, J.H. (1975): *Adaptation in Natural and Artificial Systems*. University of Michigan Press: Ann Arbor, MI.

IBC (2003): *International Building Code*. International Code Council, Falls Church, VA, 2003.

Kasai, K, and Maison, B.F. (1997): Building pounding damage during the 1989 Loma Prieta earthquake. Engineering Structures, 19 (3), 195-207

Lopez Garcia D., (2004). Separation Distance Necessary to Prevent Seismic Pounding Between Adjacent Structures. *Ph.D. Dissertation*, University at Buffalo, The State University of New York at Buffalo, Buffalo, NY.

Singh, M.P., and Moreschi, L.M. (2002): Optimal placement of dampers for passive response control. Earthquake Engineering and Structural Dynamics, 31 (4), 955-976.

3

Multihazard-Resistant Highway Bridge Pier-Bent

Shuichi Fujikura

Graduate Student, Department of Civil, Structural and Environmental Engineering, University at Buffalo

Advisor: Michel Bruneau, Professor and MCEER Director

Summary

The terrorist threat on bridges, and on the transportation system as a whole, has been recognized by the engineering community and public officials since recent terrorist attacks. Since many bridges are (or will be) located in areas of moderate or high seismic activity, and because many bridges are potential terrorist targets, there is a need to develop structural systems capable of performing equally well under both events. This paper presents the development and experimental validation of a multi-hazard bridge pier concept, i.e., a bridge pier system capable of providing an adequate level of protection against collapse under both seismic and blast loading. A multi-column pier-bent with concrete-filled steel tube (CFST) columns is the proposed concept. The work presented here experimentally investigates the adequacy of such a system under blast loading.

Introduction

Recent terrorist attacks such as the one on the Alfred P. Murrah Federal Building in Oklahoma City (1995) and the one on the tallest towers of the World Trade Center in New York City (2001) are examples of the fact that the destruction of civil engineering structures has become one of the means employed by terrorists to achieve their objectives. There are some similarities between seismic and blast effects on bridge structures: both major earthquakes and terrorist attacks/accidental explosions are rare events that can induce large inelastic deformations in the key structural components of bridges. Since many bridges are (or will be) located in areas of moderate or high seismic activity, and because many bridges are potential terrorist targets, there is a need to develop structural systems capable of performing equally well under both events.

The objective of this research project is to develop a multi-hazard bridge pier concept capable of providing an adequate level of protection against collapse under both seismic and blast loading, and whose members' dimensions are not very different from those currently found in typical highway bridges. This paper describes design of the multi-hazard bridge pier-bent under blast and seismic loading, and experiments of 1/4 scale of the prototype bridge pier-bent. Additionally, the results from the blast experiments are compared with the ones from a simplified method of analysis considering an equivalent SDOF system having an elastic-perfectly-plastic behavior.

Design of Multihazard Bridge Pier-bent

Preliminary work included the examination of several different structural configurations of bridge piers and potential bridge bent systems, to identify some systems deemed most appropriate in

meeting the objectives of this research. In all cases, bents were assumed part of a typical 3-span continuous highway bridge located in an area of moderate seismic activity.

A pier-bent design concept consisting of concrete-filled steel tube columns (CFST columns) linked by a cap-beam proved to be more satisfactory, and was found possible using available tube sections (Bruneau and Marson, 2004; Marson and Bruneau 2004). It was found that material effectiveness was highest for piers having the highest diameter-to-thickness (D/t) ratio. CFST columns with cross-sections of 16" diameter were found to provide adequate blast and seismic resistance during the design process. These CFST columns are smaller than the typical 3'-diameter reinforced concrete pier column, but expected to perform significantly better under blast loads. This type of structural member was deemed likely to be accepted in practice. This structural configuration was therefore selected for experimental verification of its blast resistance.

Experiments on 1/4 Scale Multihazard Bridge Pier-bent

A series of tests was performed at U.S. Army Corps of Engineers Research Facility in Vicksburg, Mississippi. Due to constraints in the maximum possible blast charge weight that could be used at the test site, test specimen dimensions were set to be 1/4 scale of the prototype bridge piers.

Piers were CFST columns linked by a cap-beam and at the footing level. As indicated above, preliminary analyses showed this type of piers capable of providing high resistance and ductility against both blast and seismic loads. Experimental specimen is shown in Figure 1 and two identical specimens (Bent 1 and Bent 2) were constructed to be tested. Each specimen consists of three piers with different diameters (D = 4", 5" and 6"), connected to a steel beams embedded in the cap-beam and a foundation beam. Fiber reinforced concrete was used for the cap-beam and the foundation beam to control cracking, which was deemed desirable against spalling of the concrete due to either earthquake or blast loading. Summary of the pier tests is presented in Table 1. Exact values of charge weights and stand off distances were omitted for security reason; instead these values were expressed by W and X, respectively in Table 1.

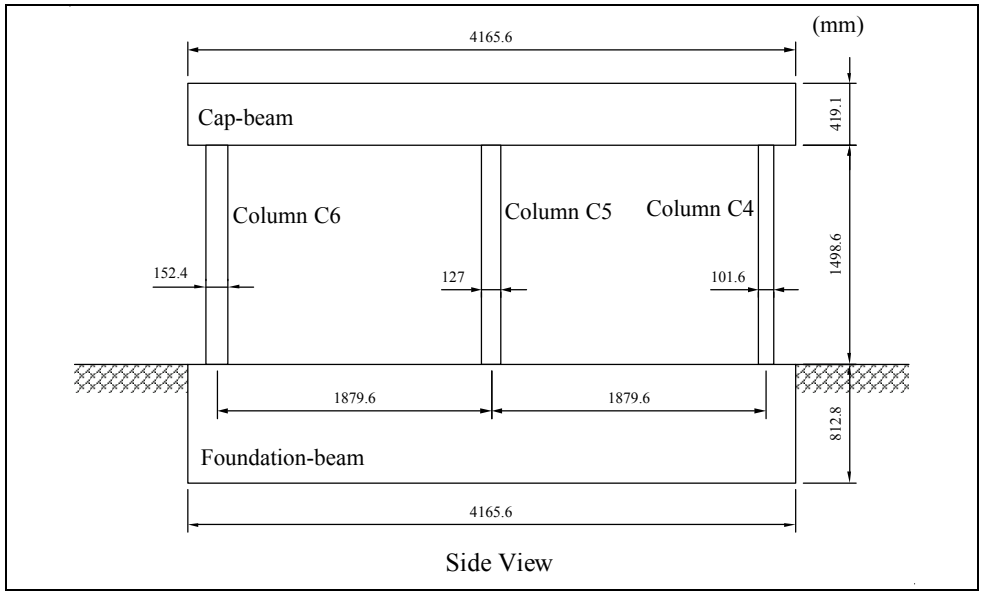

Figure 1. Experimental Specimen

Table 1. Summary of Column Test Cases, Test Results and Shape Factors

Test No.	Bent	Column	Charge Weight	X	Z[m]	Maximum Deformation [mm]
Test 1	B1	C4	0.1 W	3 X	0.250	0.0
Test 2	B1	C4	0.55 W	3 X	0.750	0.0
Test 3	B1	C4	W	2 X	0.750	30
Test 4	B1	C6	W	1.1 X	0.750	46
Test 5	B1	C5	W	1.3 X	0.750	76
Test 6	B2	C4	W	1.6 X	0.250	24
Test 9	B2	C6	W	0.8 X	0.250	45
Test 10	B2	C5	W	0.8 X	0.250	100

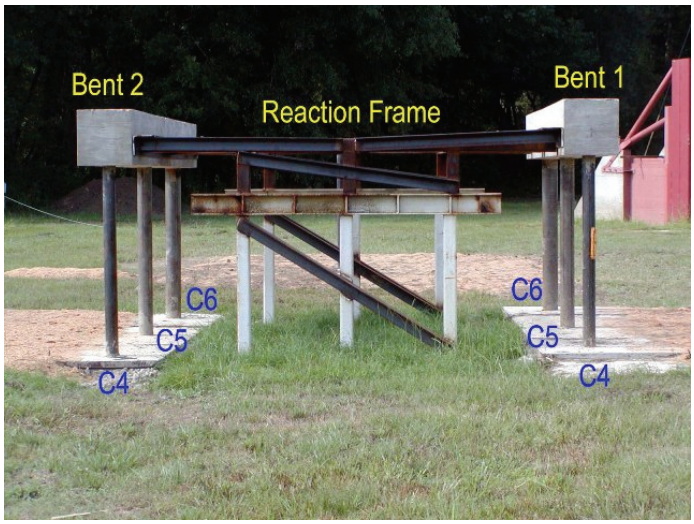

Figure 2. Test Setup

Figure 3. Column B1-C5 after Test 5

The experimental setup is shown in Figure 2. It consists of identical Bent 1 and Bent 2, and reaction frames between the two bents. Individual piers in each bent (Figure 1) were subjected to successive blast tests. Note that the cap-beams were not fixed to the reaction frames as it was intended to allow rotating to replicate actual conditions in bridges.

Maximum residual plastic deformations of each pier after testing are shown in Table 1. Figure 3 shows Column 5 of Bent 1 after the test as an example. The CFST column exhibited a ductile behavior under blast load. Note that no significant damage was suffered by the fiber reinforced concrete cap-beam as a result of the blast pressures.

Simplified Analysis for Blast Loading

The simplified procedure adopted is described in USDA (1990). The method considers an equivalent SDOF system having an elastic-perfectly-plastic behavior, and assumes that all the energy imparted to the system by the blast loading is converted into internal strain energy. Under these conditions, the maximum deformation due to impulsive-type blast loading is given by:

$$X_m = \frac{1}{2}\left(\frac{I_{eq}^2}{K_{LM}\ m\ R_u} + X_E \right) \tag{1}$$

where I_{eq} is equivalent uniform impulse per unit length, K_{LM} is load-mass factor, m is the mass per unit length of the column, R_u is the strength per unit length of the column and X_E is the displacement at the onset of plastic behavior. In this analysis, I_{eq} was calculated by:

$$I_{eq} = \beta\ D\ i_{eq} \tag{2}$$

where i_{eq} is equivalent uniform impulse per unit area, D is column diameter and β is factor to account for the reduction of pressures on the column due to its circular shape. The values of i_{eq} were calculated using the program BEL (USACE-ERDC, 2004). BEL is a shock-wave propagation program using analytical/empirical models.

Comparison with Simplified Analysis for Tests

Experimentally obtained maximum plastic deformations of the piers were compared with the ones that can be calculated using simplified method of analysis. These simplified analyses were conducted using the strength values obtained from the compression tests of concrete cylinders and the tensile tests for the steel tubes from which the specimens were constructed. Note that the maximum deformations measured after the tests were obtained without loading on the structure (i.e. after the blast load) and are actually residual plastic deformations, X_{test}. Therefore, the test results had to be compared with the calculated residual deformations whose values were $X_m - X_E$, where X_E and X_m respectively represent the elastic maximum deformations and the maximum deformations under blast loading.

Following this approach by calibrating analysis with the test results, values for β for each test were calculated using the above equations. The resulting values for β are presented in Table 1 for the six test cases for which residual plastic deformation were obtained, along with the calculated elastic maximum deformations, the calculated maximum deformations under blast loadings, and the residual plastic deformations from the tests. It was found that the value of β for this type of circular columns is 0.45 (i.e. mean value of 0.450 and standard deviation of 0.020 from the six samples considered).

Table 2. Summary of Column Test and Analysis Results and Shape Factors

Test Num	Column	Shape Factor, β	Calculation			Test
			Maximum Elastic Deformation, X_E	Maximum Deformation, X_m	Maximum Residual Deformation, $X_m - X_E$	Maximum Residual Deformation X_{test}
			[mm]	[mm]	[mm]	[mm]
Test 3	B1-C4	0.472	6	36	30	30
Test 4	B1-C6	0.458	4	50	46	46
Test 5	B1-C5	0.447	3	79	76	76
Test 6	B2-C4	0.465	10	34	24	24
Test 9	B2-C6	0.440	6	51	45	45
Test 10	B2-C5	0.417	5	105	100	100

Conclusions

This paper has presented the findings of research to establish a multi-hazard bridge pier concept capable of providing an adequate level of protection against collapse under both seismic and blast loading. A series of experiments on 1/4 scale multi-hazard bridge piers was performed. The CFST column exhibited a ductile behavior under blast load, and no significant damage was suffered by the fiber reinforced concrete cap-beam as a result of the blast pressures. The results of the blast experiments were compared with the results from simplified method of analysis considering an equivalent SDOF system. Comparison of the results of these blast tests with this simplified analysis showed that a reduction factor accounting for the reduction of pressures on the circular column resulted in a value of 0.45.

Acknowledgements

This research was carried out under the supervision of Dr. Michel Bruneau, and supported by the Federal Highway Administration under contract number DTFH61-98-C-00094 to the Multidisciplinary Center for Earthquake Engineering Research. However, any opinions, findings, conclusions, and recommendations presented in this paper are those of the authors and do not necessarily reflect the views of the sponsors.

References

Bruneau M, Marson J. (2004): Seismic design of concrete-filled circular steel bridge piers. *Journal of Bridge Engineering*, 9(1), 24-34.

Marson J, Bruneau M. (2004): Cyclic testing of concrete-filled circular steel bridge piers having encased fixed-based detail. *Journal of Bridge Engineering*, 9(1), 14-23.

USACE-ERDC (2004): *Bridge Explosive Loading (BEL) version 1.1.0.3*. US Army Corps of Engineers' Engineer Research and Development Center, Vicksburg, MS. (distribution limited to U.S. Government agencies and their contractors).

USDA (1990): Structures to Resist the Effects of Accidental Explosions. *Technical Manual TM 5-1300*, US Department of the Army, Washington, DC.

4

Application of Fragility-Based Decision Support Methodologies

Cagdas Kafali

Ph.D. Candidate, School of Civil and Environmental Engineering, Cornell University

Advisor: Mircea Grigoriu, Professor of Structural Engineering

Summary

A method is presented for assessing the seismic performance of acute care facilities and selecting optimal rehabilitation strategies for increasing the seismic resilience of these facilities. The seismic performance is measured by fragility surfaces, that is, the probability of system failure as a function of magnitude and site-to-source distance, consequences of system damage/failure, and system recovery time following earthquakes. The input to the analysis consists of system properties, seismic hazard, performance criteria, rehabilitation strategies, and a lifetime. MCEER West Coast Demonstration Hospital is used to demonstrate the method. Statistics are obtained for lifetime losses and recovery times corresponding to different rehabilitation strategies and an optimal rehabilitation strategy is selected using these statistics.

Loss Estimation Method

The proposed method is based on (i) seismic hazard analysis, (ii) fragility analysis and (iii) lifetime capacity/cost estimation (Kafali and Grigoriu 2005a). Figure 1 shows a chart summarizing the method.

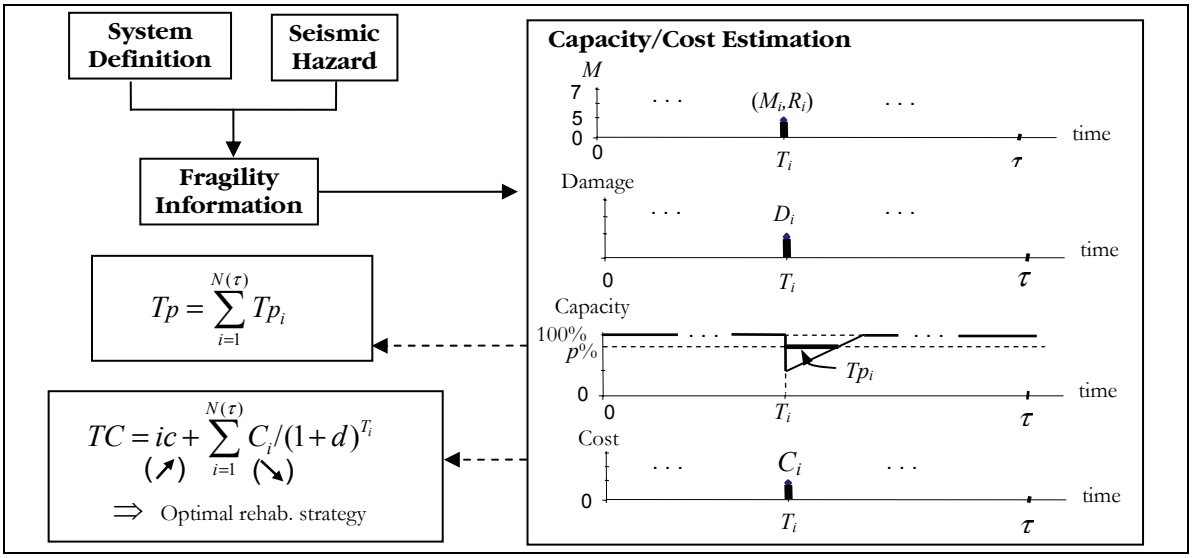

Figure 1. Loss estimation method.

In Figure 1, T_i is the arrival time of the seismic event i with moment magnitude M_i and source-to-site distance R_i, τ is the lifetime, $N(\tau)$ is the total number of seismic events in τ, Tp_i is the time the system operates below p% capacity after event i, Tp is the total time the system operates below p% capacity in τ, ic is the rehabilitation cost, C_i is the cost related to event i including costs of repair/replacement, capacity losses and life losses due to the damage in structural and nonstructural systems, TC is the total cost in τ and d is the discount rate. More information can be found in (Kafali and Grigoriu 2005a).

System Definition

A simple 2 dimensional model is used for representing the structural system of the MCEER West Coast Demonstration Hospital. More information on the model is in (Kafali and Grigoriu 2006a). Three nonstructural systems are considered in this study.

- HVAC system: It is assumed that the HVAC system consisted of two identical water chillers attached to the roof of the building. Response of these chillers to the roof accelerations are obtained using a 3 dimensional nonlinear model presented in Fathali and Filiatrault (2006).

- Piping system: The topology and the components of the sanitary water supply system are obtained using the architectural drawings of the demonstration hospital (see Table 1). Only the pipes with a diameter greater than or equal to one inch are considered.

Table 1. Piping system.

Floor	Length [ft]	Connections	Valves	Hangers
1	330	45	15	33
2	510	115	40	51
3	510	115	40	51
4	270	60	25	27

- Partition walls: The topology of the partition wall system is obtained using the architectural drawings of the demonstration hospital (see Table 2). It is assumed that all the walls between the rooms and between the rooms and the corridors are of the same type.

Table 2. Partition walls.

Floor	Walls	Effected # of beds						
		0	**1**	**2**	**3**	**4**	**5**	**6**
1	80	80	0	0	0	0	0	0
2	80	33	14	18	7	6	1	1
3	60	20	2	28	2	8	0	0
4	80	80	0	0	0	0	0	0

It is assumed that (i) cascade analysis applies, *i.e.*, the nonstructural systems do not affect the dynamics of the structural system, and (ii) systems are brought to their initial state after each event.

Rehabilitation alternatives:

- Structural system: Three alternative designs, with (i) the same stiffness as the existing system and (ii) linear viscous dampers resulting in the first mode damping ratios of 20, 25 and 30%, for the alternatives 1, 2 and 3, respectively, are considered. The dampers are inserted in the central bay in each storey of the exterior moment-resisting frame. The total rehabilitation costs for the alternatives 1, 2 and 3 are \$109,000; \$133,000 and \$180,000, respectively (Kafali and Grigoriu 2006a).

- Nonstructural systems: Rehabilitation is applied to the piping system only using bracing the system at each hanger location. The total cost of piping rehabilitation is $120,000 (Kafali and Grigoriu 2006a).

Seismic Hazard

The demonstration hospital is in Northridge, CA (118.52° West, 34.24° North) (Wanitkorkul and Filiatrault 2005) and is located on stiff soil i.e., NEHRP site class D (FEMA 273 1997). The lifetime τ is 50 years. Figure 2 shows the seismic activity matrix at the site, providing the mean annual rate of earthquakes with different (m,r). The specific barrier model (Halldorsson and Papageorgiou 2005) is used to model the strong ground motion process at the site. A Monte Carlo algorithm can be developed for generating (i) random samples of the seismic hazard at the site during a given period of time τ using the seismic activity matrix, and (ii) seismic ground acceleration samples for these seismic hazard samples. Each seismic hazard sample is defined by the number of earthquakes during the time τ, temporal distribution, and magnitude and source-to-site distance of each of them. More information on seismic hazard analysis can be found in Kafali and Grigoriu (2003a, 2005a).

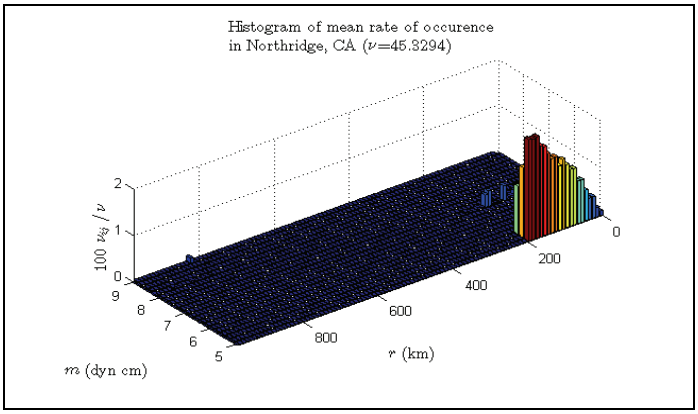

Figure 2. Seismic activity matrix for Northridge, CA.

Fragility Information

Seismic fragility analysis of structural/nonstructural system is described in detail in Kafali and Grigoriu (2003b, 2006b). Table 3 shows the damage/limit states and sample fragility surfaces for the structural/nonstructural systems considered in this study. Damage states for the structural system, HVAC equipment, piping system and partition walls are provided in FEMA 356 (2000), ASHRAE (2003), Goodwin (2004), McMullin and Merrick (2002), respectively. More information on calculating the fragility surfaces for the systems in this benchmark problem can be found in Kafali and Grigoriu (2006a).

Capacity/Cost Estimation

Capacity, for example acute care bed per day capacity, and total cost are estimated for the case of no rehabilitation and for the three rehabilitation alternatives. Using these estimates efficient solutions can be determined. The total capacity of the demonstration hospital is 93 acute care beds (43 on the 2nd floor and 50 on the 3rd floor). The net revenue per bed is $1,500/day. The cost due to a seismic event relates to (i) structural/nonstructural repair or replacement, (ii) loss of capacity in services, and (iii) loss of life. Table 4 shows the repair/replacement costs and consequences corresponding to each damage state for the structural and nonstructural systems. It is assumed that there are 150 people in the hospital when an earthquake occurs, the probability that a person losses his/her life is 0.1 and the value of life $2,200,000/person.

Table 3. Damage/limit states and sample fragility surfaces for the structural/nonstructural systems.

<table>
<tr><th>System</th><th>Damage states</th><th>Sample fragility surface</th></tr>
<tr><td>Structure</td><td>
<table>
<tr><th>Damage state</th><th>Max story drift (%)</th></tr>
<tr><td>Immediate occupancy</td><td>< 0.7</td></tr>
<tr><td>Life safety</td><td>[0.7, 2.5)</td></tr>
<tr><td>Collapse prevention</td><td>[2.5, 5.0)</td></tr>
<tr><td>Collapse</td><td>≥ 5.0</td></tr>
</table>
</td><td>structure = no rehab, ds ≥ 3
 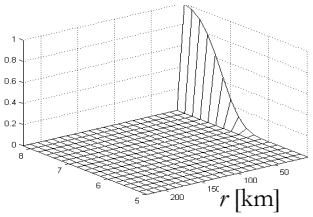
</td></tr>
<tr><td>HVAC equipment</td><td>
<table>
<tr><th>Damage state</th><th>Max total acc. (g)</th></tr>
<tr><td>No</td><td>< 2.0</td></tr>
<tr><td>Moderate</td><td>[2.0, 4.0)</td></tr>
<tr><td>Extensive</td><td>≥ 4.0</td></tr>
</table>
</td><td>structure = no rehab, ds ≥ 2
 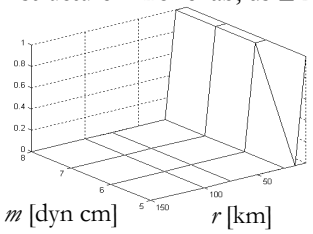
</td></tr>
<tr><td>Piping</td><td>
<table>
<tr><th rowspan="2">Damage state</th><th colspan="2">Max storey drift (%)</th></tr>
<tr><th>Existing</th><th>Rehab.</th></tr>
<tr><td>Slight</td><td>< 1.1</td><td>< 2.2</td></tr>
<tr><td>Moderate</td><td>[1.1, 2.2)</td><td>[2.2, 5.0)</td></tr>
<tr><td>Extensive</td><td>≥ 2.2</td><td>≥ 5.0</td></tr>
</table>
</td><td>structure = no rehab, ds ≥ 2
 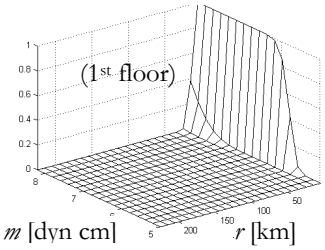
</td></tr>
<tr><td>Partition wall</td><td> 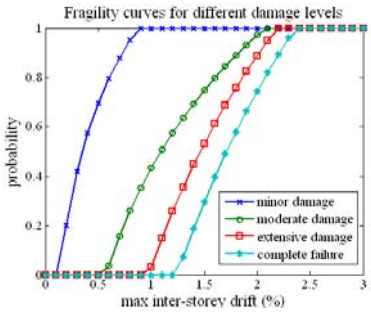
</td><td>structure = no rehab, ds ≥ 1
 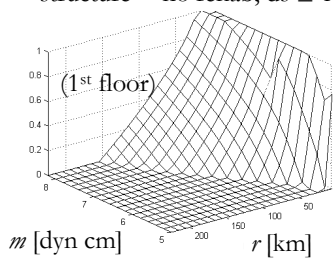
</td></tr>
</table>

Table 4. Repair/replacement costs and consequences due to damage in structural/nonstructural systems.

<table>
<tr><th>System</th><th>Repair/replacement costs and consequences</th></tr>
<tr><td>Structure</td><td>
<table>
<tr><th>Damage state</th><th>Repair/replacement cost</th><th>Consequences</th></tr>
<tr><td>Immediate occupancy</td><td>$ 280,000</td><td>Hospital is 100% operational</td></tr>
<tr><td>Life safety</td><td>$ 1,512,000</td><td>2 years repair w/ 5% capacity loss</td></tr>
<tr><td>Collapse prevention</td><td>$ 67,500,000</td><td>4 years of reconstruction</td></tr>
<tr><td>Collapse</td><td>$ 67,500,000</td><td>4 years of reconstruction</td></tr>
</table>
</td></tr>
<tr><td>HVAC equipment</td><td>
<table>
<tr><th>Damage state</th><th>Repair/replacement cost per HVAC</th><th>Consequences per HVAC</th></tr>
<tr><td>No</td><td>$ 0</td><td>No capacity losses</td></tr>
<tr><td>Moderate</td><td>$ 90,000</td><td>50% beds lost for 2 days</td></tr>
<tr><td>Extensive</td><td>$ 500,000</td><td>50% beds lost for 20 days</td></tr>
</table>
</td></tr>
<tr><td>Piping</td><td>
<table>
<tr><th>Damage state</th><th>Repair/replacement cost per wall</th><th>Consequences per wall</th></tr>
<tr><td>No</td><td>$ 0</td><td>No capacity losses</td></tr>
<tr><td>Minor</td><td>$ 230</td><td>Beds unavailable for 1 day</td></tr>
<tr><td>Moderate</td><td>$ 460</td><td>Beds unavailable for 2 days</td></tr>
<tr><td>Extensive</td><td>$ 690</td><td>Beds unavailable for 3 days</td></tr>
<tr><td>Complete failure</td><td>$ 920</td><td>Beds unavailable for 3 days</td></tr>
</table>
</td></tr>
<tr><td>Partition wall</td><td>
<table>
<tr><th rowspan="2">Damage state</th><th colspan="4">Repair/replacement cost per floor</th><th rowspan="2">Consequences per floor</th></tr>
<tr><th>1</th><th>2</th><th>3</th><th>4</th></tr>
<tr><td>Slight</td><td>$1,100</td><td>$1,690</td><td>$1,690</td><td>$900</td><td>No capacity losses</td></tr>
<tr><td>Moderate</td><td>$1,720</td><td>$4,380</td><td>$4,380</td><td>$2,290</td><td>10% beds lost for 7 days</td></tr>
</table>
</td></tr>
</table>

System Resilience and the RDAT

Rehabilitation decision analysis toolbox (RDAT) is a MATLAB based program for calculating the seismic resilience of structural/nonstructural systems in a health care facility. Using the RDAT it is possible to (i) compare the effectiveness of different rehabilitation alternatives for structural and nonstructural systems using the estimates of life cycle losses, and (ii) develop rational rehabilitation alternatives for increasing the seismic resilience of these systems. RDAT version 1 is limited to linear single degree of freedom structural/nonstructural systems and is available on the MCEER Users Networks at *http://civil.eng.buffalo.edu/users_ntwk/index.htm*. RDAT version 2 extends to linear multi degree of freedom systems and is presented in detail in Kafali and Grigoriu (2005b). The final version of the RDAT with an application to the MCEER West Coast Demonstration hospital will be made available to the MCEER Users Networks by Fall 2007.

Figure 3 shows the histograms of the (a) total time Tp the system operates below 90% capacity in 50 years, and (b) total cost TC in 50 years, for the base system and the three rehabilitation alternatives, calculated by Monte Carlo simulation using 1000 samples.

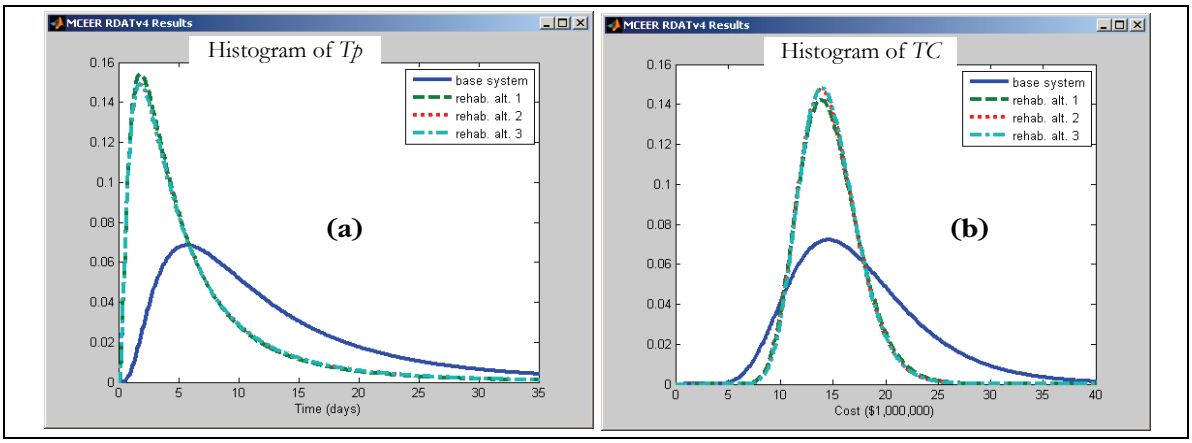

Figure 3. Histograms of *Tp* and *TC*.

Figure 4 shows $P(Tp>t)$ and $P(TC>c)$. A possible measure for comparing the effectiveness of different rehabilitation alternatives can be the probability that the total time the system operates below 90% capacity exceeds a level t_{cr} (or similarly, the probability that the total cost exceeds a level c_{cr}). Accordingly, the optimal solution is the one with the lowest $P(Tp>t_{cr})$ (or $P(TC>c_{cr})$) and depends on the selected value of t_{cr} (or c_{cr}). For example, Figure 4 shows that the optimal solutions are rehab. alt. 1, 2 and 3 for t_{cr} = 30 days (or rehabilitation alternative 3 for c_{cr} = $20,000,000).

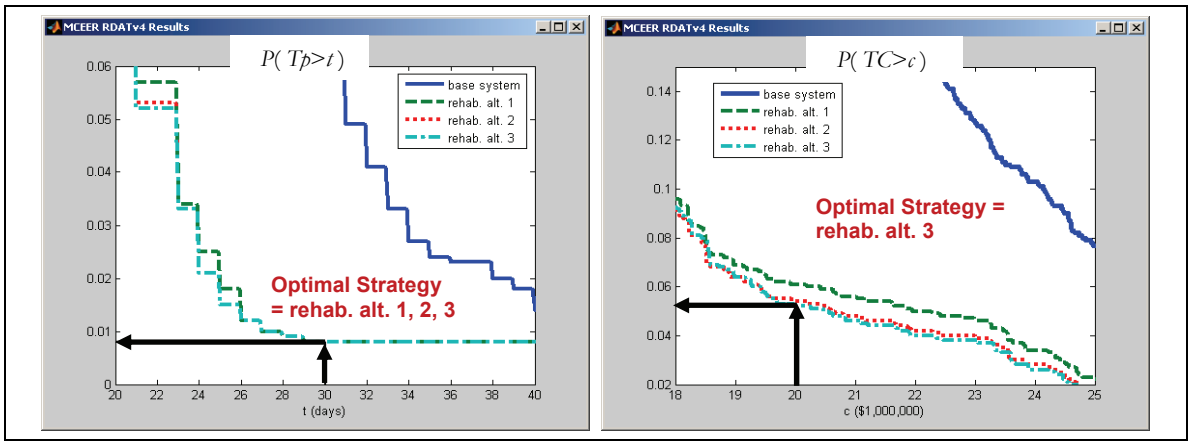

Figure 4. Optimal rehabilitation strategy.

Concluding Remarks

A method was developed to identify an optimal retrofitting technique for structural/nonstructural systems. The method (i) considers a realistic seismic hazard model rather than using the maximum credible earthquake, (ii) includes all components of costs, that is, the costs related to the structural failure and downtime, retrofitting, repair, loss of capacity in services, and loss of life, and (iii) is designed for individual facilities rather than a large population of them. The method is based on

Monte Carlo simulation, probabilistic seismic hazard, fragility surfaces and capacity/cost analyses and is applied to the MCEER West Coast Demonstration Hospital.

Acknowledgements

This research was carried out under the supervision of Professor Mircea Grigoriu, and primarily supported by the Earthquake Engineering Research Centers Program of the National Science Foundation, under award number EEC-9701471 to the Multidisciplinary Center for Earthquake Engineering Research. Contributions from A. Bansal (Degenkolb), F. Case (Clark), Dr. Filiatrault (University at Buffalo), J. Lewis (Terra Firm), R.J. Love (Degenkolb), Dr. Maragakis (University of Nevada, Reno), P. Marks (York International), J. Massey (ISAT), J. Mitchell (York International), R. Omens (NHMC, CWU), R. Rozanski (NHMC, CWU), A. Taylor (KPFF), D.P. Taylor (Taylor Devices) and Dr. Winterfeldt (University of Southern California) are greatly acknowledged.

References

ASHRAE (2003): ASHRAE Handbook - HVAC Applications. American Society of Heating, Refrigerating and Air-Conditioning Engineers, Atlanta, GA.

Fathali S., Filiatrault A. (2006): Restrained and isolated nonstructural components (RINC) Ver.1.01. *Technical Manual (in preparation)*, Multidisciplinary Center for Earthquake Engineering Research, The State University of New York at Buffalo, Buffalo, NY.

FEMA 273 (1997): NEHRP guidelines for the seismic rehabilitation of buildings, Federal Emergency and Management Agency, Washington, DC.

FEMA 356 (2000): Prestandard and commentary for the seismic rehabilitation of buildings. Federal Emergency and Management Agency, Washington, DC.

Goodwin E. (2004): Experimental evaluation of the seismic performance of hospital piping subassemblies. *M.S. Thesis*, University of Nevada. Reno, NV.

Halldorsson B., Papageorgiou A.S. (2005): Calibration of the specific barrier model to earthquakes of different tectonic regions. *Bulletin of the Seismological Society of America*, 95 (4), 1276-1300.

Kafali C., Grigoriu M. (2006a): Application of fragility-based decision support methodologies. *Technical Report (in preparation)*, Multidisciplinary Center for Earthquake Engineering Research, The State University of New York at Buffalo, Buffalo, NY.

Kafali C., Grigoriu M. (2006b): Seismic fragility analysis: Application to simple linear and nonlinear systems. *Earthquake Engineering and Structural Dynamics (in review).*

Kafali C., Grigoriu M. (2005a): Rehabilitation decision analysis. *In proceedings of the ICOSSAR'05*, Rome, Italy.

Kafali C., Grigoriu M. (2005b): Rehabilitation decision analysis toolbox. *In proceedings of the SEAOC'05*, San Diego, CA.

Kafali C., Grigoriu M. (2003a): Non-Gaussian model for spatially coherent seismic ground motions. *In proceedings of the ICASP9,* San Francisco, CA.

Kafali C., Grigoriu M. (2003b): Fragility analysis for nonstructural systems in critical facilities. *In proceedings of ATC-29-2 seminar*, Newport Beach, CA.

McMullin K.M., Merrick D. (2002): Seismic performance of gypsum walls - Experimental test program. *CUREE Wood-frame Project Report W-15*, CUREE, Richmond, CA.

Wanitkorkul A., Filiatrault A. (2005): Simulation of strong ground motions for seismic fragility evaluation of nonstructural components in hospitals. *Technical Report MCEER-05-0005*, Multidisciplinary Center for Earthquake Engineering Research, The State University of New York at Buffalo, Buffalo, NY.

5

Experimental Study of a Controlled Rocking Bridge Pier

Michael Pollino

Ph.D. Candidate, Department of Civil, Structural and Environmental Engineering, University at Buffalo

Advisor: Dr. Michel Bruneau, Professor and Director of MCEER

Summary

Controlled rocking of steel braced frames has been proposed for the seismic retrofit of structures. The controlled rocking approach allows a frame to uplift from its support at the base-of-column to foundation interface while displacement-based steel yielding devices are implemented at the base location to control the response. Past studies have focused on analytical investigations of the response of such a system along with design applications for controlled rocking bridge piers. This paper discusses shake table testing of a 4-legged, steel braced pier representative of a 1/5 length scale highway bridge pier. The model is subjected to a series of seismic excitations about one of its primary orthogonal axes, using horizontal and vertical base motions, and rotated 45deg. to investigate pier behavior that would be expected from bi-directional horizontal base inputs. Ground motions from the 1940 El Centro and 1994 Northridge earthquakes are used along with a synthetically generated motion. The steel yielding devices used during testing are triangular plates that yield in flexure as the pier uplifts and rocks at its base. Results of testing focus on overall behavior of the controlled rocking pier including global hysteretic response, uplifting displacements, and pier forces.

Introduction

The developments of seismic protective systems that provide nonlinear elastic behaviour and prevent damage to a structure's primary members have recently received increased interest. This is in part due to a growing appreciation for the ability of such systems to efficiently withstand seismic demands elastically (without damage) or directing damage to easily replaceable structural "fuses". These types of systems can often also be designed to provide a self-centering ability. This behaviour has been achieved through post-tensioning of structural members (Mander and Cheng 1997; Christopoulos et al., 2002; Garlock et al., 2005). However it may also be achieved by simply allowing structures to uplift from their foundation while preventing sliding, creating a rocking response. The seismic behaviour of conventional structural systems, such as special moment-resisting frames, concentrically braced frames, and eccentrically braced frames (AISC 2005), can be satisfactory from a life safety point of view (FEMA 2003), however damage to members can leave the structure unusable until costly repairs can be made.

In order to complement the system otherwise free to uplift, Pollino and Bruneau (2007) have proposed a controlled rocking approach for seismic resistance in which passive energy dissipation devices are added at the uplifting location to control the rocking response of steel braced frames. The devices considered were displacement-based steel yielding elements that could be calibrated to achieve a desired level of response. The cyclic hysteretic behavior including P-Δ effects and a

capacity-based design method were developed. The design method used a number of design constraints including limiting maximum displacements, impact velocity, and maximum dynamic forces such that the structure could remain elastic and self-center following excitation. Simplified methods of analysis were used to predict system response. Parametric studies, that used nonlinear time history analyses, were performed to evaluate the design and simplified analysis methods.

In order to further investigate the dynamic rocking response of controlled rocking steel braced frames, an experimental study was conducted using a 5 degree-of-freedom (5DOF) shake table in the Structural Engineering and Earthquake Simulation Laboratory (SEESL) at the University at Buffalo (UB). A 1/5 length scale specimen, representative of a 4-legged steel braced highway bridge pier was used during testing. The model was subjected to a series of seismic excitations about one of it's primary axes (θ=0deg.), using horizontal and vertical base motions, and rotated 45deg. (θ=45deg.) to investigate behavior that would be expected from bi-directional horizontal base inputs. Triangular steel plates that yield in flexure were used as the passive energy dissipation devices during testing.

Specimen Properties

It was desired to have the largest scaled model reasonably possible given the available resources in the laboratory (table size, capacity; vertical clearance). Prototype properties are based on a brief review of drawings of existing bridges supported on steel truss piers (Pollino and Bruneau 2004). Model scale was ultimately controlled by the vertical distance from the shake table to a workable crane clearance height (Figure 1). This led to a length scale factor of approximately 5 based on the prototype height of 30.3m. Other scale factors were determined following an artificial mass simulation scaling law.

The primary similitude requirements targeted were the "fixed-base" lateral and vertical periods of vibration of the model (T_{om} and T_{Lm}), the shearing mode period of vibration (T_{vm}), and the applied and restoring forces of the model which are controlled primarily by the added mass. Although an added mass of 69.4kN/g is required by similitude, steel plates totaling 75.2kN/g were used since they were readily available in the laboratory. Connection of the mass to the pier was made through 16-9.5mm fully-tensioned, high-strength threaded rods through the 2-90mm thick steel mass plates, a double concave hardened steel bearing, mild-steel connection plate, and 2-19.1mm plate washers. The connection was designed to transfer shear force in the horizontal plane and vertical forces and moments between the mass and pier.

Modifications were made at the base of the specimen to create the boundary conditions to allow the rocking response. Angles surrounded the base plate of each pier leg that were designed to transfer the horizontal shear forces in bearing however no resistance to vertical uplift was provided through this connection except for friction that may occur along an angle's leg as the pier leg uplifts. The angles were bolted to the top of large load cells that were attached to the shake table.

Steel yielding devices with bi-linear hysteretic behavior were designed with connections to only provide a vertical force to the base of the pier legs. The important design quantities for the devices are the plastic device force (V_p), elastic stiffness (k_e), and maximum allowable vertical displacement. Different steel yielding devices were considered for experimental testing including buckling-restrained braces (AISC 2005) and shear panel devices (Zahrai and Bruneau 1999). However, scaling

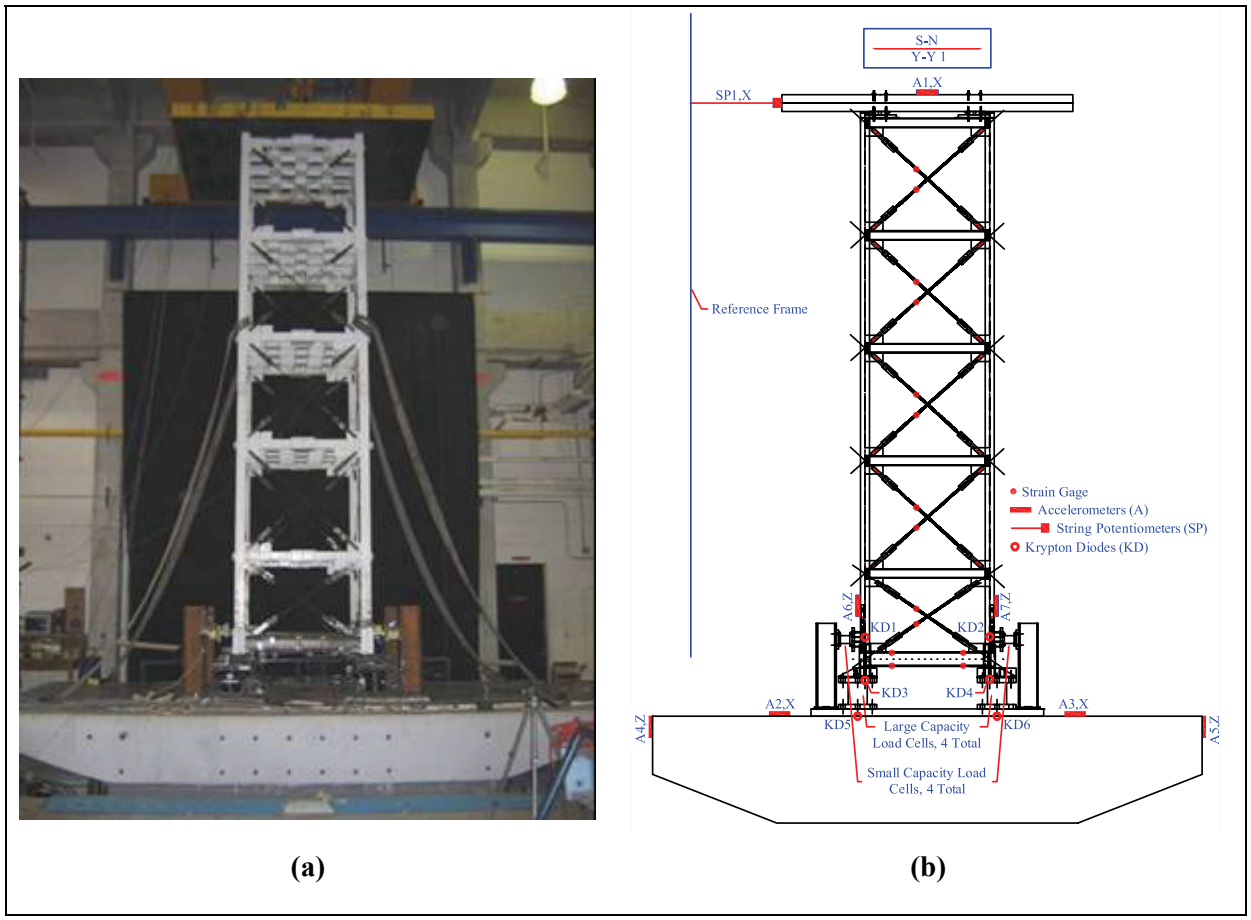

Figure 1. Experimental Pier Specimen (a) Picture of Specimen on Shake Table and (b) Instrumentation Layout

both the braces and shear panels resulted in devices that were not easily and reliably manufactured or fabricated. The number of design parameters for TADAS devices (Tsai et al., 1993) resulted in dimensions of a device that could be fabricated at this scale. Devices were designed with local strength ratios (η_L) of 1.0, 0.67, and 0.33 and to undergo a rotation ($\Delta=\Delta_{up}/L_{TADAS}$) of 0.15rad. during testing. The local strength ratio,η_L, is defined as:

$$\eta_L = \frac{V_p}{w/4} \tag{1}$$

Experimental Facilities and Instrumentation

The experimental testing was performed on the 5-DOF shake table in the SEES Laboratory at UB. The table has a nominal capacity of 20-tons with an acceleration of 1.15g and 2.30 g in the horizontal and vertical directions respectively. The table is driven by 2 horizontal and 4 vertical

hydraulic actuators that are programmable with feedback control to simultaneously control displacement, velocity, and acceleration.

The instrumentation used included accelerometers, string potentiometers, 8 strain gauge based load cells, and strain gauges that were attached onto the specimen. A Krypton K600 high performance dynamic mobile coordinate measurement machine that uses 3 cameras and LEDs is used to measure displacements near the base of the structure. The instrumentation layout for the experiments is shown in Figure 1b.

Table Input

The input excitation to the shake table included banded white noise excitation and three seismic ground motion histories. The banded white noise tests were performed to identify elastic dynamic characteristics of the model. The white noise excitation had frequency content in the range of 0-50Hz and had a PGA of approximately 0.05g. The seismic input included ground motions from the 1940 El Centro earthquake (Array #9), 1994 Northridge earthquake (Newhall), and a synthetically generated record. The pseudo-acceleration response spectrums from these three motions, in model scale are shown in Figure 2.

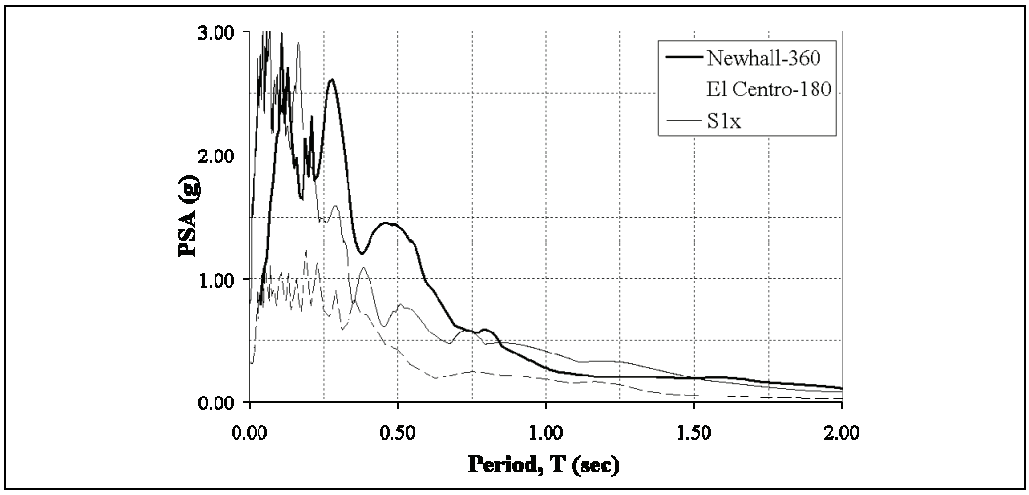

Figure 2. Target Pseudo-Spectral Acceleration Spectra for 3 Seismic Inputs

Experimental Testing Results

A sample set of results are presented in Figure 3 for the case with η_L=0.67, θ=0deg. and subjected to the synthetic record amplitude scaled by 1.5. The pier relative displacement was calculated using the string potentiometers at the top of the pier (total displacement) and the Krypton diodes on the table (table displacement and rotation). The maximum relative displacement was observed to be approximately 100mm however no residual displacement was present at the end of the test. The global hysteretic response of the pier shows the "flag-shaped" behavior and significant fluctuation in the base shear due to the excitation of the vertical "shearing" mode of vibration. Pier leg axial force histories, recorded from large capacity load cells, are shown for the two legs on the South and North end of the specimen. The TADAS hysteretic behavior was recorded from small capacity load cells and relative vertical displacements between Krypton diodes. The device rotation is calculated as the

relative vertical deformation across the device divided by the device length. No damage was visually observed within the pier specimen following testing (only inelastic behavior in the ductile "fuses"). Also, white noise testing revealed no change in the specimen's dynamic properties from test to test.

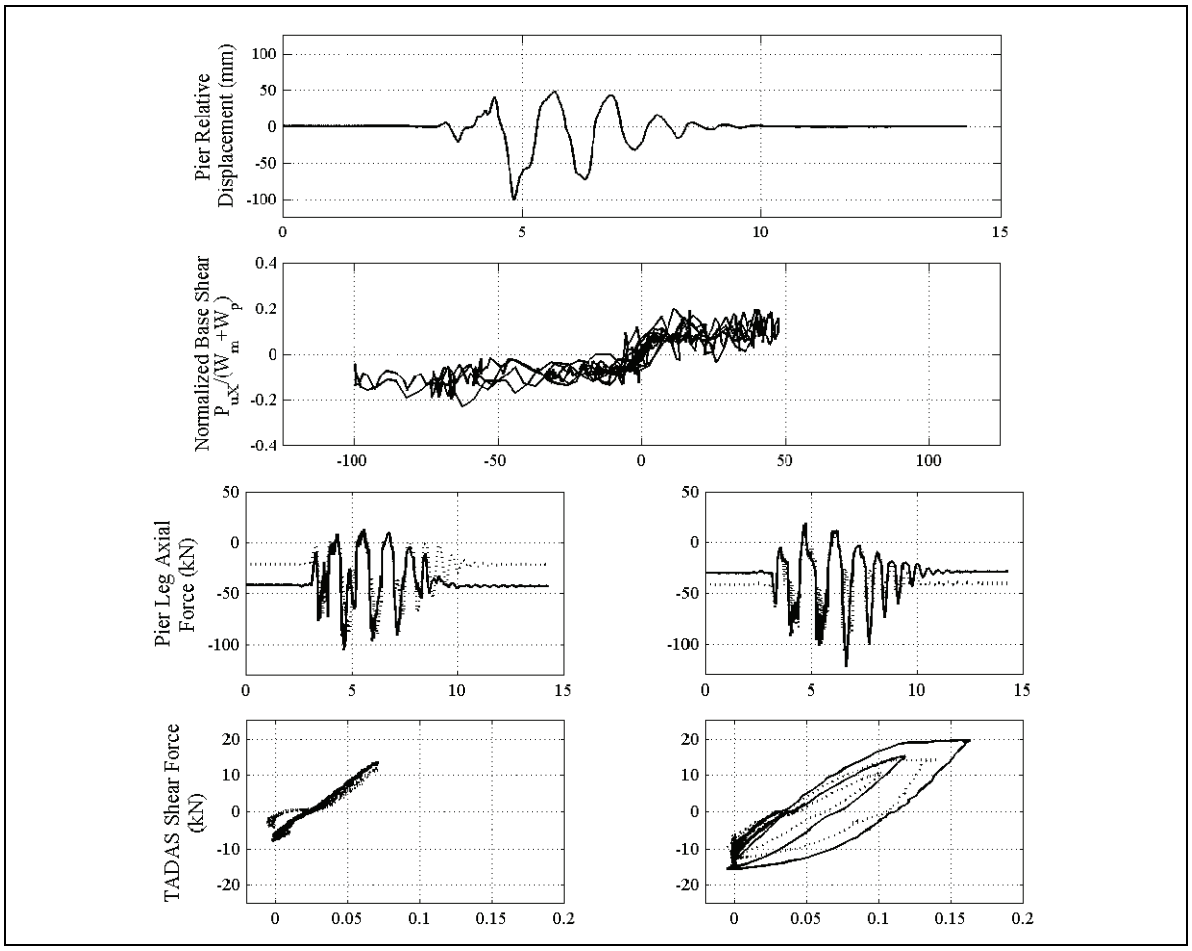

Figure 3. Experimental Testing Results (θ=0deg., η_L=0.67, Syn-150%)

Conclusions

An innovative approach for the seismic resistance of steel braced frame structures that allows uplift and rocking of braced frame structures at the foundation support has been investigated here through dynamic shake table testing. A 1/5 length scale model of a steel braced highway bridge pier was constructed and tested under strong seismic shaking. Experimental results of the controlled rocking model bridge pier demonstrated stable, elastic behavior of the pier while all damage was forced into the easily replaceable ductile structural "fuses". The simplified methods of analysis used for design were shown to provide conservative estimates of response with reasonable accuracy.

Future Research

A second phase of experimental testing is planned for early spring 2007 on one of the 6-DOF shake tables in SEESL. This phase of testing will include bi-directional horizontal input along with vertical

excitation and also investigate the use of nonlinear viscous dampers along with steel yielding devices as the passive energy dissipating devices. Further analytical studies are planned to investigate system response of bridges supported on braced steel bride piers that allow controlled rocking of the more slender piers to seismically protect the bridge. Also, finite element analysis will be used to study the issue of dynamic, pulse buckling near the base of pier legs.

Acknowledgements

This research was supported in part by the Federal Highway Administration under contract number DTFH61-98-C-00094 to the Multidisciplinary Center for Earthquake Engineering Research. However, any opinions, findings, conclusions, and recommendations presented in this paper are those of the author and do not necessarily reflect the views of the sponsors.

References

AISC (2005): Seismic Provisions for Structural Steel Buildings. ANSI/AISC 341-05, American Institute of Steel Construction, Inc., Chicago, Illinois.

Christopoulos, C., Filiatrault, A., Uang, C., and Folz, B. (2002): Posttensioned Energy Dissipating Connections for Moment-Resisting Steel Frames. J. Struct. Eng. ASCE, 128(9), 1111-1120.

FEMA (2003): *FEMA 450 NEHRP Recommended Provisions for Seismic Regulations for New Buildings and Other Structures*. Building Seismic Safety Council for the Federal Emergency Management Agency, Washington, DC.

Garlock, M., Ricles, J., and Sause, R. (2005): Experimental Studies of Full-Scale Posttensioned Steel Connections. J. Struct. Eng. ASCE, 131(3), 438-448.

Mander, J. and Cheng, C. (1997): Seismic Resistance of Bridge Piers Based on Damage Avoidance Design. *Technical Report NCEER-97-0014, National Center for Earthquake Engineering Research*, The State University of New York at Buffalo, Buffalo, NY.

Pollino, M. and Bruneau, M. (2004): Seismic Retrofit of Bridge Steel Truss Piers Using a Controlled Rocking Approach. *Technical Report MCEER-04-0011, Multidisciplinary Center for Earthquake Engineering Research,* The State University of New York at Buffalo, Buffalo, NY.

Pollino, M. and Bruneau, M. (2007): Seismic Retrofit of Bridge Steel Truss Piers Using a Controlled Rocking Approach. J. Bridge Eng. ASCE (In press).

Tsai, K.C., Chen, H.W., Hong, C.P., and Su, Y.F. (1993); Design of Steel Triangular Plate Energy Absorbers for Seismic-Resistant Construction. *Earthquake Spectra*, EERI, Vol. 9, No. 3, pp. 505-528.

Zahrai, S.M. and Bruneau, M. (1999): Cyclic Testing of Ductile End Diaphragms for Slab-on-Girder Steel Bridges. J. Struct. Eng. ASCE, 125(9), 987-996.

6

Experimental Investigation of Full Scale Two-story Steel Plate Shear Wall

Bing Qu

Ph.D. Student, Department of Civil, Structural and Environmental Engineering, University at Buffalo

Advisor: Michel Bruneau, Professor and Director of MCEER

Summary

In order to address the replaceability of the infill panels following an earthquake and the seismic behavior of intermediate beams, a two-phase experimental program was carried out on a full scale two-story steel plate shear wall with reduced beam section connections and composite floors. In Phase I the specimen was pseudo-dynamically tested subjected to three ground motions of progressively decreasing intensity. In Phase II, the buckled panels were replaced by new panels prior to subjecting the specimen to subsequent pseudo-dynamic and cyclic tests until failure. It is shown that the repaired specimen can survive and dissipate significant amounts of hysteretic energy in a new earthquake without severe damage to the boundary frame or overall strength degradation. It is also found that the specimen had exceptional redundancy and exhibited stable displacement-force behavior for drifts up to 5.2% and 5.0% at the first and second story, respectively.

Introduction

Steel plate shear walls (SPSW) consist of steel panels surrounded by boundary frame members. These panels are allowed to buckle in shear and subsequently form a diagonal tension field. SPSW are progressively being used as the primary lateral force resisting systems in buildings (Sabelli and Bruneau 2006). Past monotonic, cyclic and shaking table tests on SPSW in United States, Canada, Japan, Taiwan and other countries have shown that this structural system can exhibit high initial stiffness, behave in a ductile manner and dissipate significant amounts of hysteretic energy (Literature reviews are available in Berman and Bruneau 2003). Analytical research on SPSW has also validated useful models for the design and analysis of this lateral load resisting system (Thorburn et al.1983; Driver et al. 1997; Berman and Bruneau 2003).

However, no research has directly addressed the replaceability of infill panels following an earthquake, and there remain uncertainties regarding the seismic behavior of intermediate beams in SPSW (intermediate beams are those to which are welded steel plates above and below, by opposition to anchor beams that have steel plates only below or above respectively). The latter problem was analytically addressed by Lopez Garcia and Bruneau (2006) using simple models, but experimental investigations on the behavior of intermediate beams, particularly for beams having reduced beam section (RBS) connections and composite concrete slabs, can provide much needed information on behavior of SPSW system and how to best design the intermediate beams. To address the above issues, a two-phase experimental program was developed to test a two-story SPSW specimen having an intermediate composite beam with RBS connections. The testing

program also investigated how to replace a steel panel after a severe earthquake and how the repaired SPSW would behave in a second earthquake. This paper summarizes the tests conducted and the observed ultimate behavior.

Specimen Description and Test Setup

A full scale two-story one-bay SPSW specimen was fabricated in Taiwan and a two-phase experimental program (Phase I and II tests) was conducted at the laboratory of the National Center for Research in Earthquake Engineering (NCREE) in Taipei, Taiwan. The specimen with equal height and width panels at each story was measured 8000mm high and 4000mm wide between boundary frame member centerlines. The infill panels and boundary frame members were sized based on the recommendations provided by Berman and Bruneau (2003). Beams and columns were of A572 Gr.50 steel members. Infill panels were specified to be SS400 steel which is similar to ASTM A36 steel in this case. The RBS connection design procedure was used to detail the beam-to-column connections at top, intermediate and bottom level respectively. The infill panels were designed to be 3mm and 2mm thick at the first and second story respectively. Prior to Phase II tests, the buckled infill panels were removed using flame-cut and replaced by new panels. Fish plates were used along boundary frame members to connect infill panels. The infill panels of Phase I were welded on one side of the fish plates and those of Phase II on the other side.

The specimen was mounted on the strong floor. In-plane (south-north) servo controlled hydraulic actuators were mounted between the specimen and a reaction wall. Based on the ultimate strength of the specimen assessed using the plastic analysis procedures (Berman and Bruneau 2003), three 1000kN hydraulic actuators were employed to apply earthquake load or cyclic load on the specimen at each story. Ancillary trusses as part of the floor slab system were used to transfer in-plane loads to the specimen at floor levels. In order to avoid out-of-plane (east-west) displacement at floor levels, two hydraulic actuators, mounted between the ancillary truss and a reaction frame, were used at floor levels. A vertical load of 1400kN was applied by a reaction beam at the top of each column to simulate gravity load. Each reaction beam transferred the load exerted from two vertical actuators mounted between the reaction beam and the anchor rods pined to the strong floor. The specimen schematic and test setup are illustrated in Figures 1a-1c. The designation of H shapes correspond to US designation W shapes reflecting the depth, flange width, as well as web and flange thicknesses.

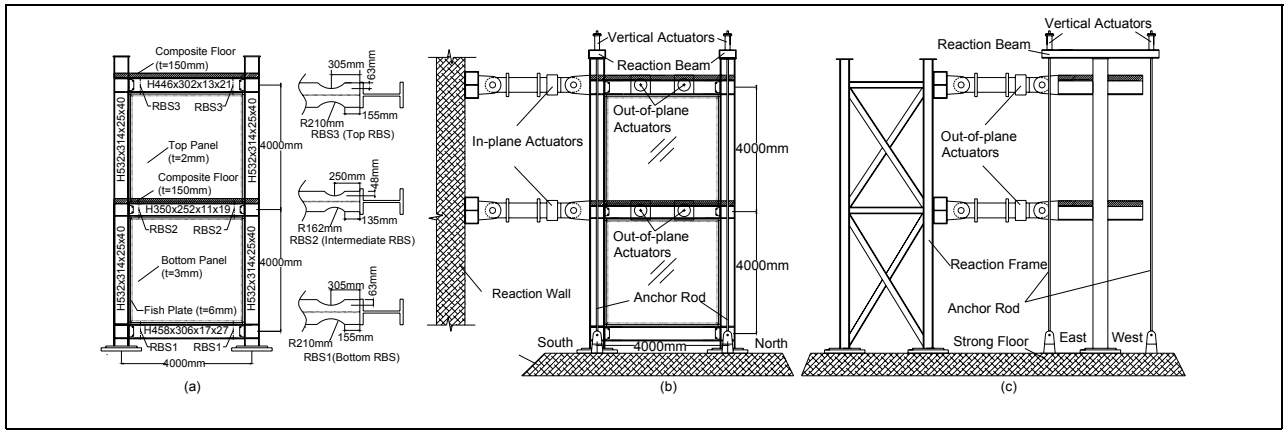

Figure 1: Specimen Schematic (a); In-plane Setup (b); Out-of-Plane Setup (c)

Phase I Tests

In Phase I, the specimen was tested under three pseudo-dynamic loads using the Chi-Chi earthquake record (TCU082EW) scaled up to levels of excitations representative of seismic hazards having 2%, 10% and 50% probabilities of exceedances in 50 years, subjecting the wall to earthquakes of progressively decreasing intensity. Despite the numerous ancillary calculations that checked the adequacy of the specimen, the intermediate concrete slab and the south column base suffered premature failures at the time step of 9.5sec. and 24sec. of the first earthquake record respectively. The tests resumed after the specimen was strengthened at these locations. The SPSW specimen behaved similarly to the Phase II pseudo-dynamic test described in greater length below. No fracture was found in the boundary frame and it was deemed to be in satisfactory condition allowing for the replacement of infill panels for the subsequent phase of testing. Detailed information about specimen design and results from the Phase I tests are presented elsewhere (Lin et al 2006).

Phase II Pseudo-dynamic Test

In order to investigate how the repaired SPSW specimen would behave in a second earthquake in the first stage of Phase II, the specimen was tested under pseudo-dynamic load corresponding to the Chi-Chi earthquake record (TCU082EW) scaled up to the seismic hazard of 2% probability of occurrence in 50 years which was equivalent to the first earthquake record considered in the Phase I tests after the buckled panels were replaced by new panels.

Figure 2a. Specimen prior to Phase II tests

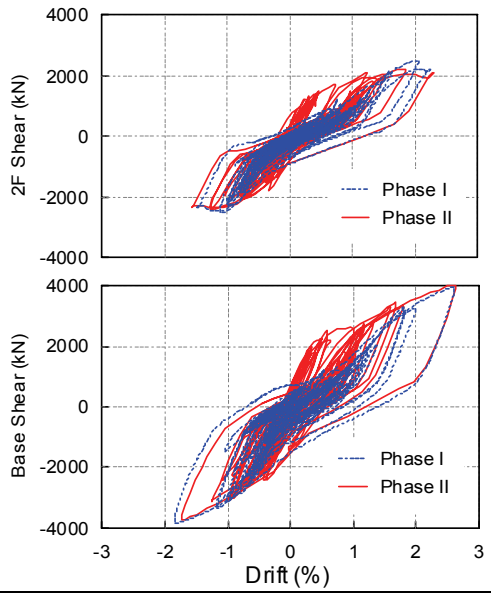

Figure 2b. Hystereses of Phase I and Phase II Pseudo-dynamic test

The specimen prior to Phase II tests and hysteretic curves from Phase II pseudo-dynamic test along with the counterpart results from Phase I are shown in Figure 2a-2b. Drifts designated as "+"or "-" refer to loading in the north and south directions respectively. Observation of the hysteretic curves obtained from the Phase II shows that the first story dissipated more hysteretic energy than the

second story. Both the first and second story exhibited stable displacement-force behavior, with some pinching of the hysteretic loops as the magnitude of drifts increased, particularly after the development of a small fracture along the bottom of the shear tab at the north end of the intermediate beam at drifts of 2.6% and 2.3% at the first and second story respectively. After the pseudo-dynamic test, the boundary frame was in good condition except for the aforementioned damage in the shear tab of the intermediate beam. There were notable plastic deformations at the column bases and RBS connections at all levels. All welds within the SPSW specimen were intact after the test. Comparing the hysteretic curves from the Phase I and Phase II tests shown together in Figure 2b, the two specimens are found to behave similarly under the same strong ground motion except that the initial stiffness of the repaired specimen is higher than that of the original one. This is because the results shown for the specimen in Phase I are those obtained after the specimen was repaired due to the unexpected failures mentioned in Phase I tests. Therefore the infill panels had already experienced some inelastic deformation before these unexpected failures occurred.

Phase II Cyclic Test

The next stage of Phase II tests involved cyclic test on the SPSW specimen in order to investigate the ultimate behavior of intermediate beam and the cyclic behavior and ultimate capacity of SPSW system after severe earthquakes. As mentioned in the observations of Phase II pseudo-dynamic test, the boundary frame members were in good condition after the pseudo-dynamic test except for a small fracture that was found along the bottom of the shear tab at the north end of the intermediate beam. To correct this limited damage and to get a better assessment of the possible ultimate capacity of SPSW, the damaged shear tab was replaced by a new one prior to conducting the cyclic test. A displacement-controlled scheme was selected for the cyclic test.

The hysteretic curves resulting from the Phase II cyclic test, along with the results of Phase II pseudo-dynamic tests described in detail in the prior section, are shown in Figure 3. It is observed the initial stiffness of the SPSW specimen in the cyclic test was smaller than that in pseudo-dynamic test. Because the previous pseudo-dynamic test stretched the infill panels up to specimen drifts of 2.6% and 2.3% at the first and second story respectively, the hysteretic loops exhibited pinching up to those drifts. Hysteretic loops were then full until drifts of 2.8% and 2.6% at the first and second story respectively in Cycle 7, when complete fracture occurred along the shear tab at the north end of the intermediate beam. A similar fracture developed along the shear tab at the south end of the intermediate beam when the specimen was pulled towards to the reaction wall in this cycle.

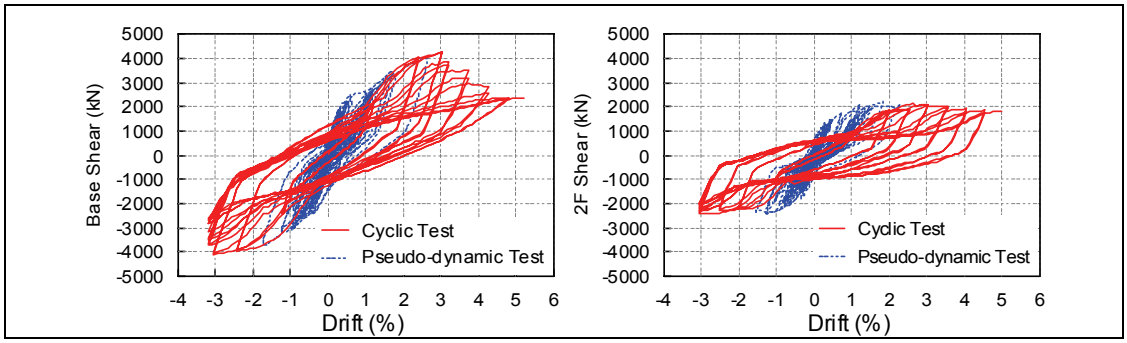

Figure 3. Hystereses of the Phase II tests

Rupture of the shear tabs triggered fracture of the bottom flange at the north end of the intermediate beam. At drifts of 3.3% and 3.1% at the first and second story respectively in Cycle 9, the bottom flange at the north end of the intermediate beam fractured as shown in Figure 4. However, no fractures developed in the reduced beam flange regions of the intermediate beam. The welds connecting the infill panels to the fish plates around the north end of the intermediate beam also fractured over a substantial length to a more severe extent after the specimen experienced drifts of 5.2% and 5.0% at the first and second story respectively as shown in Figure 5. These events significantly changed the load path within the system. However, the SPSW specimen was still able to exhibit stable displacement-force behavior as evidenced by the hysteretic curves shown in Figure 3, which demonstrates the redundancy of this kind of structural system. The cyclic test ended at drifts of 5.2% and 5.0% at the first and second story respectively, when a sudden failure occurred in the load transfer mechanism, i.e. when a fatal longitudinal crack developed along the top concrete slab of the specimen as shown in Figure 6.

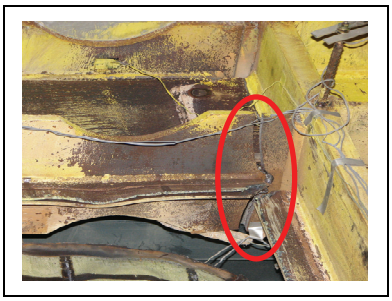

Figure 4. Ruptures at the north end of intermediate beam

Figure 6. Crack at the top slab

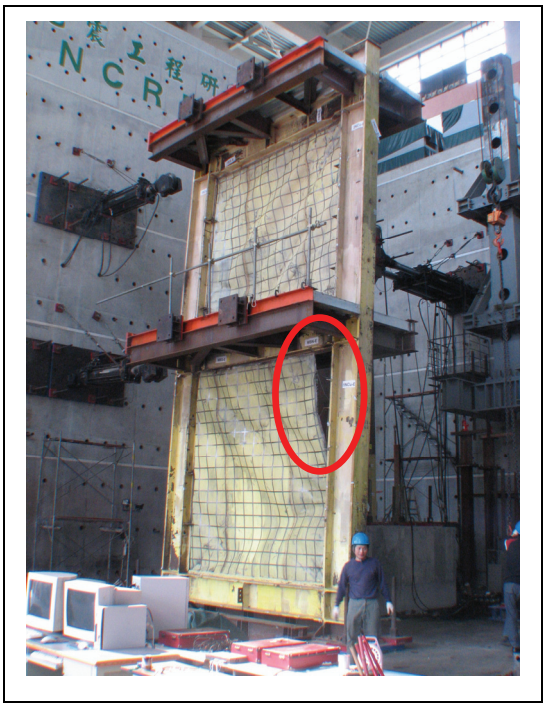

Figure 5. Fracture of the welds connecting the infill panels to fish plates

Concluding Remarks

A full scale two-story SPSW specimen was designed and investigated in a two-phase experimental program. The pseudo-dynamic tests show that a SPSW repaired by replacing the infill panels buckled in a prior earthquake by new ones can be a viable option to provide adequate resistance to the lateral loads imparted on this structure during new seismic excitations (note that possible undesirable aesthetic issues related to the residual drifts prior to replacing the panels are beyond the scope of this work). The repaired SPSW behaved quite similarly to the original one. Testing showed that the repaired SPSW can survive and dissipate a similar amount of energy in the subsequent earthquake without severe damage to the boundary frame and without overall strength degradation.

Results from the cyclic test allowed to investigate the ultimate displacement capacity of the SPSW specimen. Though the hysteretic curves were pinched at low drift levels due to the inelastic deformations that the infill panels experienced during the pseudo-dynamic test, and even though the strength of the SPSW dropped as the ends of the intermediate beam fractured, the SPSW structure exhibited stable displacement-force behavior and provided a significant energy dissipation capacity, exhibiting substantial redundancy.

The columns and anchor beams, as well as top and bottom RBS connections performed as intended. However, the intermediate beams failed unexpectedly. The ends of the intermediate beams having RBS connections ultimately developed fractures in the shear tabs followed by fractures at the end of the bottom beam flange. No fractures developed in the reduced beam flange region. Further investigation is required to clarify the local behavior of intermediate beams in SPSW, to allow developing a better understanding of how such intermediate beams should be designed.

Acknowledgements

This research was carried out under the supervision of Prof. Michel Bruneau, and primarily supported by the Earthquake Engineering Research Centers Program of the National Science Foundation, under award number EEC-9701471 to the Multidisciplinary Center for Earthquake Engineering Research.

References

Berman, J.W., and Bruneau, M. (2003): Experimental Investigation of Light-Gauge Steel Plate Shear Walls for the Seismic Retrofit of Buildings, *Technical Report MCEER-03-0001*, Multidisciplinary Center for Earthquake Engineering Research, Buffalo, NY.

Berman, J.W., and Bruneau, M. (2003): Plastic Analysis and Design of Steel Plate Shear Walls. *Journal of Structural Engineering*, 129(11), 1448-1456.

Driver R.G., Kulak G.L., Kennedy, D.J.L., and Elwi A.E. (1997): Seismic Behavior of Steel Plate Shear Walls. Structural Engineering Report No.215, University of Alberta, Edmonton, Alberta, Canada.

Lin, C.H., Tsai, K.C., Lin, Y.C., Wang, K.J., Hsieh, W.D., Weng, Y.T., Qu, B., and Bruneau, M. (2006): The Sub-structural Pseudo-dynamic Tests of A Full-scale Two-story Steel Plate Shear wall. *Proceeding of the 4th International Conference on Earthquake Engineering. Paper No.155*, Taipei, Taiwan.

Lopez-Garcia, D. and Bruneau, M. (2006): Seismic Behavior of Intermediate beams in Steel Plate Shear Walls, *Proceeding of the 8th U.S. National Conference on Earthquake Engineering, Paper No.1089,* San Francisco, CA.

Sabelli, R., and Bruneau, M. (2006): *Steel Plate Shear Walls (AISC Design Guide)*, American Institute of Steel Construction, Chicago, Illinois.

Thorburn, L.J., Kulak, G.L. and Montgomery C.J. (1983): Analysis of Steel Plate Shear Walls. *Structural Engineering Report No. 107*, Department of Civil Engineering, The University of Alberta, Edmonton, Alberta, Canada.

Production Staff

- Jane E. Stoyle, Managing Editor
- Michelle A. Zuppa, Layout and Design
- David Pierro, Graphics and Cover Design

Cover Images

Cover Images (from top left, then clockwise): MCEER SLC Participants at the Wellington Hospital Construction Site during the *2006 Tri-Center Field Mission to New Zealand*; A shear plate shear wall specimen prior to testing, along with a hysteresis diagram (p. 39) from Bing Qu's paper, *Experimental Investigation of Full Scale Two-story Steel Plate Shear Wall*; A schematic of the overall framework of evolutionary methodology (p.11) from Seda Dogruel's paper, *Evolutionary Seismic Design and Retrofit with Application to Adjacent Structures*; MCEER SLC students (from left): Mohammad Reza Bayat, Mehdi Ahmadizadeh, Xiaoyun Shao, Macarena Schachter, Hyong Uk Kim, Gian Paolo Cimellaro at the May 2007 *ASCE Structures Congress* held in Long Beach, California; A graph from Seda Dogruel's paper, *Evolutionary Seismic Design and Retrofit with Application to Adjacent Structures*, showing a damped spectrum of ground motion records from the MCEER Northridge earthquake ensemble (p.10); MCEER SLC Participants, (from left): Bing Qu, Seda Dogruel, Nurhan Ecemis and Georgios Apostolakis, at E-Defense facilities in Miki City during the *2007 Tri-Center Field Mission to Japan*; A photo of an experimental pier specimen on a shake table with instrumentation layout diagram (p.33) from Michael Pollino's paper, *Experimental Study of a Controlled Rocking Bridge Pier;* A photo showing a post-test fracture of the welds connecting the infill panels to fish plates (p. 41), from Bing Qu's paper, *Experimental Investigation of Full Scale Two-story Steel Plate Shear Wall*; MCEER SLC members Saeed Fathali, University at Buffalo, Seda Dogruel, University at Buffalo and Cagdas Kafali, Cornell University at the Student Poster Session of the *2006 MCEER Annual Meeting* in Washington DC.

Acknowledgements

This work was supported primarily by the Earthquake Engineering Research Centers Program of the National Science Foundation under NSF Award Number EEC-9701471.

Any opinions, findings and conclusions or recommendations expressed in this material are those of the author(s) and do not necessarily reflect those of the National Science Foundation.

EARTHQUAKE ENGINEERING TO EXTREME EVENTS

University at Buffalo, The State University of New York
Red Jacket Quadrangle ▪ Buffalo, New York 14261
Phone: (716) 645-3391 ▪ Fax: (716) 645-3399
E-mail: *mceer@buffalo.edu* ▪ WWW Site *http://mceer.buffalo.edu*

University at Buffalo *The State University of New York*